Gene 578 (2016) 38–51

Contents lists available at ScienceDirect

Gene

journal homepage: www.elsevier.com/locate/gene

Research paper

The impact of oil spill to lung health—Insights from an RNA-seq study of human airway epithelial cells

Yao-Zhong Liu [a,*], Astrid M. Roy-Engel [b,c], Melody C. Baddoo [c,d], Erik K. Flemington [c,d], Guangdi Wang [e], He Wang [f,**]

[a] Dept. of Biostatistics and Bioinformatics, Tulane University School of Public Health and Tropical Medicine, New Orleans, LA, USA
[b] Dept. of Epidemiology, Tulane University School of Public Health and Tropical Medicine, New Orleans, LA, USA
[c] Tulane Cancer Center, Tulane University, New Orleans, LA, USA
[d] Dept. of Pathology, Tulane University School of Medicine, New Orleans, LA, USA
[e] Dept. of Chemistry, Xavier University of Louisiana, New Orleans, LA, USA
[f] Dept. of Chronic Respiratory Diseases, School of Health Sciences, University of Newcastle, Callaghan, Australia

ARTICLE INFO

Article history:
Received 19 November 2015
Accepted 7 December 2015
Available online 9 December 2015

Keywords:
BP oil spill
Oil dispersants
RNA-seq
Lung health
Airway epithelial cells

ABSTRACT

The Deepwater Horizon oil spill (BP oil spill) in the Gulf of Mexico was a unique disaster event, where a huge amount of oil spilled from the sea bed and a large volume of dispersants were applied to clean the spill. The operation lasted for almost 3 months and involved >50,000 workers. The potential health hazards to these workers may be significant as previous research suggested an association of persistent respiratory symptoms with exposure to oil and oil dispersants. To reveal the potential effects of oil and oil dispersants on the respiratory system at the molecular level, we evaluated the transcriptomic profile of human airway epithelial cells grown under treatment of crude oil, the dispersants Corexit 9500 and Corexit 9527, and oil-dispersant mixtures. We identified a very strong effect of Corexit 9500 treatment, with 84 genes (response genes) differentially expressed in treatment vs. control samples. We discovered an interactive effect of oil-dispersant mixtures; while no response gene was found for Corexit 9527 treatment alone, cells treated with Corexit 9527 + oil mixture showed an increased number of response genes (46 response genes), suggesting a synergic effect of 9527 with oil on airway epithelial cells. Through GO (gene ontology) functional term and pathway-based analysis, we identified upregulation of gene sets involved in angiogenesis and immune responses and downregulation of gene sets involved in cell junctions and steroid synthesis as the prevailing transcriptomic signatures in the cells treated with Corexit 9500, oil, or Corexit 9500 + oil mixture. Interestingly, these key molecular signatures coincide with important pathological features observed in common lung diseases, such as asthma, cystic fibrosis and chronic obstructive pulmonary disease. Our study provides mechanistic insights into the detrimental effects of oil and oil dispersants to the respiratory system and suggests significant health impacts of the recent BP oil spill to those people involved in the cleaning operation.

1. Introduction

The Gulf of Mexico oil spill (aka the Deepwater Horizon oil spill or BP oil spill) is considered the largest accidental marine oil spill in the history of the petroleum industry. During the event that lasted for almost 3 months, a huge amount of oil spilled from the sea bed and over 1.8 million gallons of dispersants (mainly Corexit 9500 and Corexit 9527) was applied (Hayworth and Clement, 2012; Kujawinski et al., 2011). More than 50,000 workers were involved in the oil clean-up process. The spilled crude oil, dispersants, or oil-dispersant mixture that can be inhaled as aerosols created a potential significant health threat to these workers.

The oil-dispersant mixtures contain potentially mutagenic/carcinogenic chemicals including PAH, benzene, and benzene derivatives (Rodrigues et al., 2010; Saeed and Al-Mutairi, 1999). Previous studies revealed that exposure to oil spills can cause persistent respiratory

Abbreviations: RNA-seq, RNA-sequencing; WAF, Water Accommodated Fraction; GEO, Gene Expression Omnibus; DAVID, Database for Annotation, Visualization, and Integrated Discovery; GO, Gene ontology; KEGG, Kyoto Encyclopedia of Genes and Genomes; SP-PIR, Protein information resource; GAGE, Generally Applicable Gene-set Enrichment for Pathway Analysis; BH, Benjamini–Hochberg; PAMR1, Peptidase domain containing associated with muscle regeneration 1; COPD, Chronic obstructive pulmonary disease.

* Correspondence to: Y-Z Liu, Dept. of Biostatistics and Bioinformatics, Tulane University School of Public Health and Tropical Medicine, 1440 Canal Street, Suite 2001, New Orleans, LA 70112, USA.
** Correspondence to: H Wang, Dept. of Chronic Respiratory Diseases, School of Health Sciences, The University of Newcastle, HA08 Hunter Building, University Drive, Callaghan, NSW 2308, Australia.
E-mail addresses: yliu8@tulane.edu (Y.-Z. Liu), he.wang@newcastle.edu.au (H. Wang).

http://dx.doi.org/10.1016/j.gene.2015.12.016
0378-1119/

symptoms (Zock et al., 2012), long-lasting airway oxidative stress (Rodriguez-Trigo et al., 2010), and systemic genetic effects (Laffon et al., 2006; Perez-Cadahia et al., 2007; Perez-Cadahia et al., 2008a; Perez-Cadahia et al., 2008b) in rescue workers. Toxicological effects have also been shown on sea life following exposure to oil-dispersant mixtures (Barron et al., 2003; Duarte et al., 2010). The use of oil dispersants was also found to increase PAH uptake by fish exposed to crude oil (Ramachandran et al., 2004).

For an initial characterization of the potential impact of oil and/or dispersants to the human respiratory system at the molecular level, we performed the first RNA-sequencing (RNA-seq) study using cultured human airway epithelial cells (the BEAS-2B cell line) as a model system that was treated with crude oil, dispersants (Corexit 9500 and Corexit 9527), and oil-dispersant mixtures (Corexit 9500 + oil and Corexit 9527 + oil). Through this analysis, we identified a number of genes (response genes) and functional terms/pathways that were differentially expressed in treated cells vs. controls, featuring enhanced expression of gene sets for angiogenesis and immune response and the reduced expression of gene sets for cell junction and steroid biosynthesis. Our study provides the first insight into the molecular signatures of the effect of oil and/or dispersants to the human respiratory system and suggests a significant health impact of oil spills to the oil-cleaning rescue workers.

2. Material and methods

2.1. Experimental design

The basic design of the experiment is illustrated in Fig. 1. Human airway epithelial cells were grown under six conditions (including control). After the treatment, the cells were processed for RNA extraction and downstream RNA-seq analysis.

2.2. Cell culture

Human bronchial epithelial cells (BEAS-2B cells, ATCC® CRL-9609™), purchased from American Type Culture Collection (ATCC, Wiltshire, USA), were cultured following standard guidelines. Thawed cells were initially grown in a pre-coated flask containing fibronectin (0.01 g/ml), bovine collagen type 1 (0.03 mg/ml), and bovine serum albumin (0.01 mg/ml). Following overnight growth in this pre-coated flask, the cells were subcultured in Dulbecco's Modified Eagle Medium (Invitrogen, Carlsbad, CA), supplemented with 10% fetal bovine serum (FBS), 100 U/ml penicillin, and 100 U/ml streptomycin (Invitrogen, Carlsbad, CA). Cells were cultured at 37 °C in a 100% humidified atmosphere of 5% CO_2 in air.

2.3. Chemicals

Louisiana Sweet Crude Oil was kindly provided by The Architecture, Engineering, Consulting, Operations and Management Company (AECOM, Los Angeles, CA). This oil was obtained from the site of the Macondo well during the BP oil spill disaster. Commercially available Corexit EC9500A and EC9527 dispersants were kindly provided by a contract between Nalco/Exxon Energy Chemicals, L.P. (Sugar Land, TX, USA) and Tulane University (New Orleans, USA). The dispersants are liquid solutions ready for use.

2.4. Water Accommodated Fraction (WAF) of crude oil and dispersants

To prepare WAFs for crude oil and dispersants, the following procedure was adapted from published protocols (Hemmer et al., 2011; Major et al., 2012). First, the mixture of crude oil/dispersants with culture medium was made using the following volume ratios: (1) a 1:20 ratio (crude oil: Dulbecco's Modified Eagle Medium/10%FBS/5%PenStrep) for the WAF of crude oil only, (2) a 1:40 ratio (Corexit dispersant: Dulbecco's Modified Eagle Medium/10%FBS/5%PenStrep) for the WAF of Corexit dispersants only, and (3) a 2:1:40 ratio (crude oil: Corexit dispersant: Dulbecco's Modified Eagle Medium/10%FBS/5%PenStrep) for WAF-dispersed oil (oil-dispersant mixture). Second, the resultant products were then mixed with 10 mL of deionized water with the following ratios: (1) 3% for WAF of crude oil; (2) for WAF of dispersants or oil-dispersant mixtures, a concentration of 300 ppm was used (Shi et al., 2013). The water-to-Corexit ratio is within Nalco manufacturer guidelines for dispersant application.

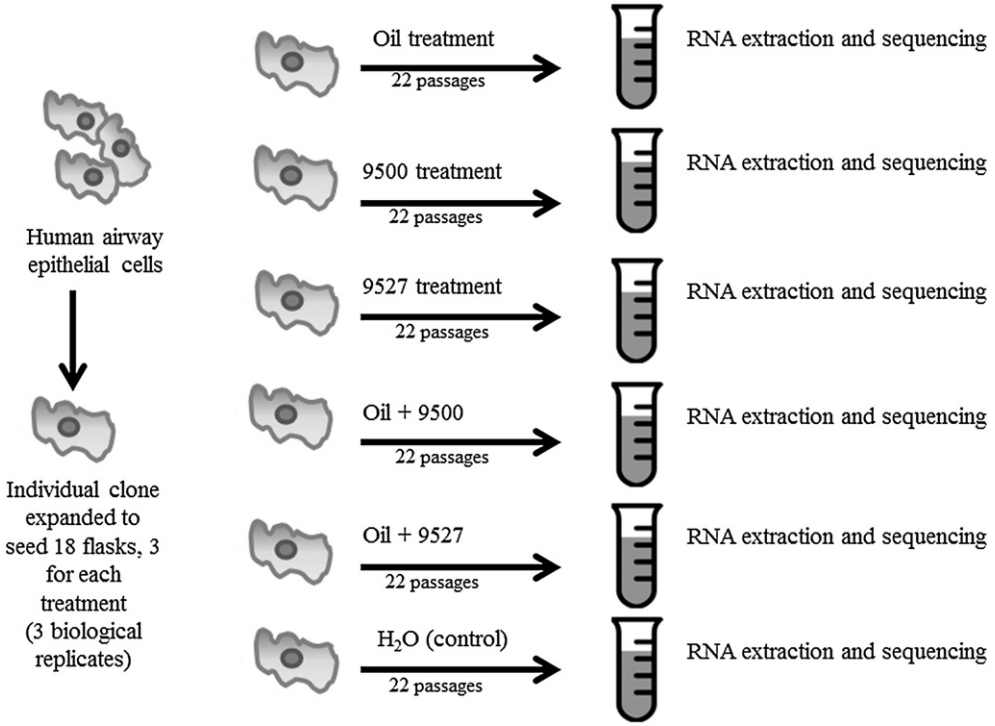

Fig. 1. Experimental design.

This final product of WAF mixed with 10 mL water was applied to a flask to treat the human airway epithelial cells (as described in the Section 2.5).

For making control (the control WAF), we followed the procedure for making WAF of crude oil but using deionized water to replace crude oil.

Each sample was stirred, with a magnetic bar, in a volumetric flask and at a rate where it was observable that the mixing volume would not exceed a vortex depth greater than 25% of the sample volume. Samples were stirred for 18 h. Once mixed, the sample was allowed to settle overnight in a separation funnel. Following overnight settling, the WAF layer was separated from the mixture, filtered with a Stericup (Millipore, USA), and stored.

2.5. Treatment of cells with WAFs of oil and dispersants

A single clone of BEAS-2B was grown to homogenize genomic variation between cultured cells. The cloned cells were divided equally into eighteen separate flasks (hence three independent replicate cell samples for each treatment evaluated) and grown for 22 passages (P22) for ~3 months under the six growing conditions (treatments) shown in Fig. 1. After the treatment, cells from each flask were shipped in dry ice to Omega Bio-Tek, Inc. (Norcross, GA), for RNA extraction, library generation, and RNA-seq analyses. For each treatment, we used the WAF of oil or dispersant or oil-dispersant mixtures made as described in Section 2.4.

2.6. RNA extraction and RNA-seq experiment

Total RNA was extracted from the eighteen individually frozen cell pellets (~8 million cells) using the E.Z.N.A. Total RNA Kit II (Omega Bio-tek, Norcross, GA) following manufacturer's instructions. Briefly, cell pellets were homogenized and lysed in RNA-Solv reagent. RNA was captured on a HiBind RNA binding column. An on-column DNase treatment step was performed before purified RNA was eluted. The concentration of the RNA was measured using a NanoDrop 2000c Spectrophotomer (Thermo Scientific, Wilmington, DE). The total RNA quality (RINe) was assessed using the RNA Screen Tape on an Agilent 2200 TapeStation instrument (Agilent Technologies, Santa Clara, CA).

Illumina TruSeq Stranded mRNA sequencing was performed by Omega Bioservices (Norcross, GA) following the standard Illumina kit protocol (Illumina, San Diego, CA). Briefly, polyA mRNA from an input of 500 ng high-quality total RNA (RINe > 8) was purified, fragmented, and first- and second-strand cDNA synthesized. Barcoded linkers were ligated to generate indexed libraries. The libraries were quantified using the Promega QuantiFluor dsDNA System on a Quantus Fluorometer (Promega, Madison, WI). The size and purity of the libraries were analyzed using the High Sensitivity D1000 Screen Tape on an Agilent 2200 TapeStation instrument. The libraries were pooled and run on an Illumina HiSeq 2500 sequencer using paired end 100 bp Rapid Run format to generate 40 million total reads per sample.

The raw RNA-seq data were submitted to Gene Expression Omnibus (GEO) and archived under an accession number GSE70909.

2.7. Data analyses

The basic data analysis scheme is illustrated in Fig. 2. The transcriptome profiles of the three independent biological replicate samples from each treatment group were compared with the three independent biological replicate samples from the control group. Based on that comparison, differential expression analysis at both single gene and functional term/gene set/pathway levels were conducted. The detailed data analysis workflow is described as follows.

The raw fastq data were adaptor-trimmed and mapped to hg19 human reference genome using the TopHat Alignment Tool (Trapnell et al., 2012) within the Illumina BaseSpace app suite (www.basespace.illumina.com) to generate the BAM files. Based on the BAM files, we then used a number of Bioconductor packages to process the BAM files into gene count matrix following the procedures listed under http://www.bioconductor.org/help/workflows/rnaseqGene/. Specifically, we used "BamFileList" function from the "Rsamtools" package (Morgan et al., 2010) to specify the number of reads (2,000,000 reads) to be processed at a time. We then used "makeTrascriptDbFromGFF" from the "GenomicFeatures" package (Lawrence et al., 2013) to generate a database object that contains annotation information of exons, transcripts, and genes from the UCSC Genome Browser. The "summarizeOverlaps" function from the "GenomicAlignments" package (Lawrence et al., 2013) was then used to annotate the bam files and generate a gene count matrix containing the gene count for each sample.

Based on this gene count matrix, we used "DESeq2" package (Love et al., 2014) to identify differentially expressed genes (response genes) between a treatment group vs. the control group. The identified differentially expressed genes at the significance level of BH-adjusted p value of 0.10 are listed in Tables 1–4. DESeq2 package requires "raw" counts of sequencing reads as the starting point for differential expression analysis (Love et al., 2014). Therefore, before submitted to the program for analysis, the count matrix was not normalized (which is explicitly required by the software) (Love et al., 2014). However, during the analysis procedures of DESeq2, normalization did occur in the modeling process, where the read count for gene i and sample $j$was modeled as a negative binomial distribution with mean μ_{ij} and dispersion α_j, and $\mu_{ij} = s_{ij}q_{ij}$, where q_{ij} is the raw read count and s_{ij} is a size factor that normalizes differences in sequencing depth between samples and other sources of technical biases, such as GC content and gene length (Love et al., 2014).

For each treatment, we selected those genes that achieved a raw p value of <0.05 in differential expression analysis and submitted those genes to DAVID (Database for Annotation, Visualization and Integrated Discovery) Functional Annotation Tool (http://david.abcc.ncifcrf.gov/summary.jsp) (Dennis et al., 2003) to annotate the genes at the levels of Gene Ontology (GO), KEGG (Kyoto Encyclopedia of Genes and Genomes), SP-PIR (protein information resource), and other functional terms/gene sets/pathways. For each treatment, the upregulated and downregulated genes were annotated separately so as to identify upregulated or downregulated functional terms/gene sets/pathways, respectively. Those terms/gene sets/pathways that achieved a Bonferroni-adjusted p value of less than 0.05 are listed in Tables 6–14.

In addition, we also submitted to DAVID (Dennis et al., 2003) functional annotation analysis those response genes shared between different treatments (as shown in Fig. 3). The annotation result is shown in Table 5.

The genes that were counted into some key prevalent functional terms (as shown in Tables 6-14), such as GO:0005912 ~ adherens junction, GO:0001568 ~ blood vessel development, and GO:0016126 ~ sterol biosynthetic process, are listed in Table 15.

We also used a Bioconductor package, GAGE (Generally Applicable Gene-set Enrichment for Pathway Analysis) (Luo et al., 2009), to identify differentially expressed gene sets or pathways in the treatment vs. the control groups. As required by the GAGE package (Luo et al., 2009) http://www.bioconductor.org/packages/release/bioc/vignettes/gage/inst/doc/RNA-seqWorkflow.pdf, the raw gene counts were first normalized with a size factor, which is calculated by the library size of each sample (sum of raw read counts for each sample) divided by the E to the power of the mean of natural logarithm-transformed library sizes across all the samples. The normalized count values were further logarithm-transformed (with a base of 2) and added with a constant number of 8 before submitted to formal GAGE analysis. GAGE is a gene-set-based analysis that tests whether the mean fold changes of a target gene set (in case vs. control groups) are significantly different from that of the background set (the whole gene set of the RNA-seq data) (Luo et al., 2009) using a test that is similar to the t test.

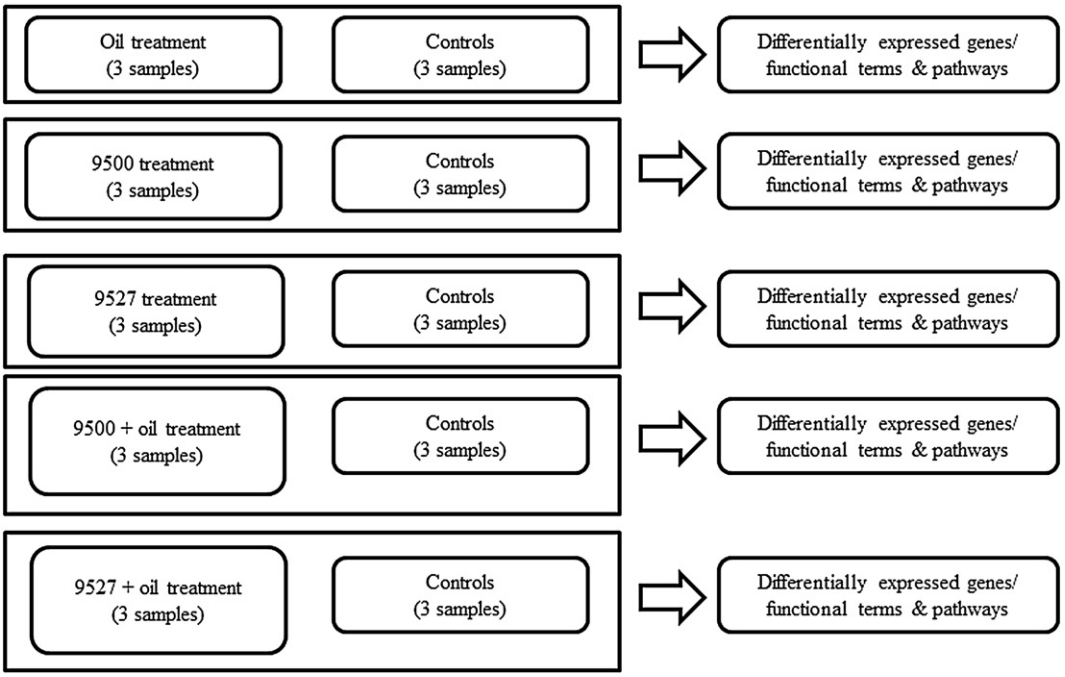

Fig. 2. Data analysis scheme.

3. Results

3.1. Differential expression analysis at the individual gene level

At significance level of Benjamini–Hochberg (BH)-adjusted p value (Benjamini and Hochberg, 1995) < 0.10, we found 26 differentially expressed genes (response genes), including 17 upregulated and 9 downregulated genes in oil treatment vs. controls (Table 1), 84 response genes (including 38 upregulated and 46 downregulated genes) in 9500 treatment (Table 2), 4 response genes (including 1 upregulated and 3 downregulated genes) in "9500 + oil" (oil-dispersant 9500 mixture) treatment (Table 3), 46 response genes (including 14 upregulated and 32 downregulated genes) in "9527 + oil" (oil-dispersant 9527 mixture) treatment (Table 4). At the significance level of BH-adjusted p value < 0.10, no gene was found differentially expressed in 9527 treatment vs. controls. The upregulation and downregulation of a gene are defined by the sign of the log2 fold change in treatment over control, with a positive sign suggesting upregulation and a negative sign downregulation (Tables 1–4).

Table 1
Response genes in oil treatment.

Ensembl ID	HGNC symbol	Raw p value	BH-adjusted p	log2 fold change
ENSG00000167995	*BEST1*	1.35E-06	6.05E-03	0.52
ENSG00000218537	*MIF-AS1*	2.23E-06	6.05E-03	0.51
ENSG00000132003	*ZSWIM4*	2.42E-06	6.05E-03	−0.48
ENSG00000149090	*PAMR1*	6.41E-06	8.82E-03	−0.44
ENSG00000109686	*SH3D19*	7.06E-06	8.82E-03	0.47
ENSG00000143882	*ATP6V1C2*	8.66E-06	9.61E-03	0.48
ENSG00000108515	ENO3	9.68E-06	9.67E-03	0.47
ENSG00000203865	ATP1A1-AS1	5.58E-05	2.99E-02	0.46
ENSG00000125730	*C3*	4.51E-05	2.99E-02	0.46
ENSG00000245970	*SNORA72*	4.92E-05	2.99E-02	0.46
ENSG00000106799	*TGFBR1*	5.00E-05	2.99E-02	−0.42
ENSG00000229124	VIM-AS1	4.33E-05	2.99E-02	0.44
ENSG00000161010	C5orf45	1.34E-04	4.88E-02	0.37
ENSG00000179362	HMGN2P46	1.35E-04	4.88E-02	−0.40
ENSG00000113070	*HBEGF*	1.81E-04	6.23E-02	−0.44
ENSG00000142627	*EPHA2*	2.72E-04	8.40E-02	−0.29
ENSG00000264577	SNORD4A	2.63E-04	8.40E-02	0.41
ENSG00000137285	*TUBB2B*	2.77E-04	8.40E-02	−0.32
ENSG00000152348	ATG10	4.44E-04	9.66E-02	0.39
ENSG00000134259	NGF	4.11E-04	9.66E-02	−0.41
ENSG00000148840	PPRC1	4.22E-04	9.66E-02	−0.33
ENSG00000116690	PRG4	3.99E-04	9.66E-02	0.42
ENSG00000237054	PRMT5-AS1	4.61E-04	9.66E-02	0.42
ENSG00000255857	PXN-AS1	4.69E-04	9.66E-02	0.40
ENSG00000157734	SNX22	4.23E-04	9.66E-02	0.39
ENSG00000105825	TFPI2	3.69E-04	9.66E-02	0.41

Note: Genes with symbols italicized are those that also responded to other treatments. BEST1, MIF, SH3D19, ATP6V1C2, C3, SNORA72, TGFBR1, and TFP12 are the response genes also for 9500 treatment. ZSWIM4, HBEGF, and EPHA2 are the response genes also for 9527 + oil treatment. PAMR1 and TUBB2B are the response genes also for 9500 and 9527 + oil treatment.

Twenty response genes under different treatments overlap (Fig. 3). In particular, downregulation of PAMR1 and TUBB2B was found in both 9500, oil, and "9527 + oil" treatments. Downregulation of COL8A1 was found in 9500, "9500 + oil," and "9527 + oil" treatments. Upregulation of BEST1, MIF, SH3D19, ATP6V1C2, C3, SNORA72, TFP12 and downregulation of TGFBR1 were found in both 9500 and oil treatments. Downregulation of ZSWIM4, HBEGF, and EPHA2 was found in both oil and "9527 + oil" treatments. Downregulation of PCSK9, KIRREL3, TAGLN and upregulation of CIR, LY6E, and WFDC2 were found in both 9500 and "9527 + oil" treatments.

We submitted the 20 shared response genes (as shown in Fig. 3) to DAVID for functional annotation. According to DAVID analysis of the 10 upregulated response genes (BEST1, MIF, SH3D19, ATP6V1C2, C3, SNORA72, TFP12, C1R, LY6E, and WFDC2), those top terms with BH-adjusted p value < 0.10 are "innate immunity," "classical complement pathway," and "immune response," with a fold of enrichment ranging from >30 to >110. The detailed annotation result is shown in Table 5.

3.2. Differential expression analysis at the functional term/gene set/pathway level

3.2.1. Downregulated terms/gene sets/pathways at the significance level of Bonferroni-corrected p value (Dunn, 1961) < 0.05

For oil treatment, 19 functional terms were downregulated (Table 6). Prevailing terms are those related to cell junctions, such as GO:0005912 ~ adherens junction, GO:0070161 ~ anchoring junction, and GO:0030055 ~ cell-substrate junction. In addition, several

Table 2
Response genes in 9500 treatment.

Ensembl ID	HGNC_symbol	Raw p value	BH-adjusted p	log2 fold change
ENSG00000149591	*TAGLN*	1.05E-13	1.05E-09	−0.79
ENSG00000144810	*COL8A1*	2.39E-11	1.20E-07	−0.67
ENSG00000169174	*PCSK9*	1.92E-10	6.44E-07	−0.73
ENSG00000125730	*C3*	5.47E-10	1.37E-06	0.71
ENSG00000130203	APOE	3.86E-08	6.46E-05	0.65
ENSG00000105825	*TFPI2*	3.76E-08	6.46E-05	0.62
ENSG00000159403	*C1R*	6.45E-08	9.27E-05	0.48
ENSG00000099998	GGT5	9.03E-08	1.14E-04	0.69
ENSG00000120708	TGFBI	1.15E-07	1.29E-04	0.46
ENSG00000149571	*KIRREL3*	2.03E-07	2.04E-04	−0.61
ENSG00000159176	CSRP1	4.81E-07	4.40E-04	−0.36
ENSG00000106799	*TGFBR1*	5.30E-07	4.44E-04	−0.58
ENSG00000184557	SOCS3	7.55E-07	5.84E-04	0.60
ENSG00000163430	FSTL1	1.47E-06	1.06E-03	−0.33
ENSG00000135636	DYSF	2.85E-06	1.82E-03	−0.57
ENSG00000140416	TPM1	3.70E-06	2.19E-03	−0.41
ENSG00000218537	*MIF-AS1*	5.20E-06	2.91E-03	0.50
ENSG00000120549	KIAA1217	1.03E-05	5.20E-03	−0.48
ENSG00000146592	CREB5	1.41E-05	6.43E-03	−0.55
ENSG00000154175	ABI3BP	1.87E-05	7.53E-03	−0.53
ENSG00000186480	INSIG1	1.80E-05	7.53E-03	−0.44
ENSG00000198959	TGM2	1.73E-05	7.53E-03	0.50
ENSG00000211445	GPX3	2.13E-05	8.24E-03	0.50
ENSG00000169047	IRS1	3.65E-05	1.35E-02	−0.42
ENSG00000121858	TNFSF10	3.75E-05	1.35E-02	0.54
ENSG00000143367	TUFT1	4.29E-05	1.49E-02	−0.43
ENSG00000108846	ABCC3	4.47E-05	1.50E-02	0.38
ENSG00000149090	*PAMR1*	4.67E-05	1.52E-02	−0.44
ENSG00000112972	HMGCS1	5.43E-05	1.56E-02	−0.48
ENSG00000101335	MYL9	5.30E-05	1.56E-02	−0.36
ENSG00000136274	NACAD	6.51E-05	1.82E-02	−0.45
ENSG00000130164	LDLR	6.77E-05	1.84E-02	−0.40
ENSG00000167995	*BEST1*	8.10E-05	2.02E-02	0.41
ENSG00000173918	C1QTNF1	8.24E-05	2.02E-02	0.48
ENSG00000134030	CTIF	7.96E-05	2.02E-02	−0.36
ENSG00000108854	SMURF2	8.07E-05	2.02E-02	−0.40
ENSG00000196954	CASP4	8.56E-05	2.05E-02	0.39
ENSG00000112851	ERBB2IP	9.63E-05	2.25E-02	−0.32
ENSG00000159388	BTG2	1.25E-04	2.85E-02	0.48
ENSG00000074416	MGLL	1.29E-04	2.89E-02	−0.42
ENSG00000113161	HMGCR	1.36E-04	2.97E-02	−0.39
ENSG00000182326	C1S	1.45E-04	3.10E-02	0.43
ENSG00000063438	AHRR	1.62E-04	3.39E-02	−0.49
ENSG00000186815	TPCN1	1.73E-04	3.47E-02	0.41
ENSG00000067064	IDI1	1.82E-04	3.51E-02	−0.38
ENSG00000196754	S100A2	1.85E-04	3.51E-02	0.43
ENSG00000135919	SERPINE2	1.84E-04	3.51E-02	0.46
ENSG00000137285	*TUBB2B*	1.95E-04	3.63E-02	−0.30
ENSG00000118849	RARRES1	2.17E-04	3.91E-02	0.47
ENSG00000245970	*SNORA72*	2.16E-04	3.91E-02	0.42
ENSG00000151702	FLI1	2.33E-04	4.12E-02	0.46
ENSG00000035403	VCL	2.64E-04	4.57E-02	−0.36
ENSG00000170458	CD14	2.98E-04	4.99E-02	0.40
ENSG00000101443	*WFDC2*	3.05E-04	5.04E-02	0.48
ENSG00000112769	LAMA4	3.48E-04	5.52E-02	0.42
ENSG00000196923	PDLIM7	3.53E-04	5.52E-02	−0.30
ENSG00000145632	PLK2	3.57E-04	5.52E-02	0.32
ENSG00000160613	PCSK7	3.73E-04	5.68E-02	−0.31
ENSG00000067082	KLF6	4.03E-04	5.71E-02	0.41
ENSG00000128422	KRT17	3.88E-04	5.71E-02	−0.36
ENSG00000109686	*SH3D19*	3.94E-04	5.71E-02	0.32
ENSG00000124107	SLPI	4.00E-04	5.71E-02	0.46
ENSG00000143882	*ATP6V1C2*	4.21E-04	5.87E-02	0.40
ENSG00000020577	SAMD4A	4.26E-04	5.87E-02	−0.39
ENSG00000225670	CADM3-AS1	4.64E-04	6.06E-02	0.41
ENSG00000131711	MAP1B	4.61E-04	6.06E-02	−0.30
ENSG00000124145	SDC4	4.61E-04	6.06E-02	−0.33
ENSG00000179820	MYADM	4.86E-04	6.19E-02	−0.34
ENSG00000160218	TRAPPC10	4.82E-04	6.19E-02	−0.36
ENSG00000157557	ETS2	5.58E-04	6.87E-02	−0.33
ENSG00000160932	*LY6E*	5.69E-04	6.89E-02	0.29
ENSG00000169710	FASN	5.98E-04	7.16E-02	−0.29
ENSG00000075702	WDR62	6.86E-04	8.03E-02	−0.32
ENSG00000230606	LOC100506123	7.17E-04	8.29E-02	−0.33
ENSG00000130513	GDF15	7.26E-04	8.29E-02	0.43

Table 2 (*continued*)

Ensembl ID	HGNC_symbol	Raw p value	BH-adjusted p	log2 fold change
ENSG00000102265	TIMP1	7.46E-04	8.44E-02	0.34
ENSG00000146072	TNFRSF21	7.70E-04	8.61E-02	0.37
ENSG00000013619	MAMLD1	7.91E-04	8.74E-02	−0.37
ENSG00000160179	ABCG1	8.43E-04	9.21E-02	0.42
ENSG00000089127	OAS1	8.55E-04	9.25E-02	0.43
ENSG00000183722	LHFP	8.76E-04	9.34E-02	−0.32
ENSG00000169180	XPO6	9.10E-04	9.53E-02	−0.26
ENSG00000110880	CORO1C	9.43E-04	9.78E-02	−0.28
ENSG00000072163	LIMS2	9.73E-04	9.98E-02	−0.40

Note: Genes with symbols italicized are those that also responded to other treatments. BEST1, MIF, SH3D19, ATP6V1C2, C3, SNORA72, TGFBR1, and TFP12 are the response genes also for oil treatment. PCSK9, KIRREL3, C1R, TAGLN, LY6E, and WFDC2 are the response genes also for 9527 + oil treatment. PAMR1 and TUBB2B are the response genes also for oil and 9527 + oil treatment. COL8A1 is the response gene also for 9527 + oil and 9500 + oil treatments.

cytoskeleton terms are also involved, *e.g.*, GO:0005856 ~ cytoskeleton, GO:0001725 ~ stress fiber, GO:0032432 ~ actin filament bundle, and GO:0042641 ~ actomyosin.

For 9500 treatment, 42 functional terms were downregulated (Table 7). Again, several terms related to cell junctions, *e.g.*, GO:0005912 ~ adherens junction and GO:0070161 ~ anchoring junction, are involved. In addition, there are terms related to sterol biosynthesis (*e.g.*, GO:0016126 ~ sterol biosynthetic process, hsa00100:Steroid biosynthesis and SP_PIR_KEYWORDS ~ Steroid biosynthesis) and terms related to cytoskeleton structure, organization, and protein binding (*e.g.*, SP_PIR_KEYWORDS ~ actin-binding, GO:0007010 ~ cytoskeleton organization, GO:0015629 ~ actin cytoskeleton).

For 9527 + oil treatment, 20 functional terms were downregulated (Table 8). The terms appear to be different from oil or 9500 treatments. The prevailing terms are those related to development and cell differentiation and proliferation, such as GO:0051094 ~ positive regulation of developmental process, GO:0045597 ~ positive regulation of cell differentiation, GO:0042127 ~ regulation of cell proliferation, GO:0008284 ~ positive regulation of cell proliferation, and GO:0043067 ~ regulation of programmed cell death.

For 9527 treatment, only one term was downregulated (Table 9), which is GO:0044421 ~ extracellular region part. For 9500 + oil treatment, three terms were downregulated (Table 10), which are SP_PIR_KEYWORDS ~ chondroitin sulfate proteoglycan, SP_PIR_KEYWORDS ~ signal, and GO:0008203 ~ cholesterol metabolic process.

3.2.2. Upregulated terms/gene sets/pathways at the significance level of Bonferroni-corrected p value (Dunn, 1961) < 0.05

For 9500 treatment, 14 terms are upregulated (Table 11). Notable terms are GO:0001568 ~ blood vessel development and GO:0001944 ~ vasculature development.

For 9500 + oil treatment, 21 terms are upregulated (Table 12). Again, several terms related to blood vessel development appear in the list, which are GO:0001568 ~ blood vessel development, GO:0001944 ~ vasculature development, GO:0001525 ~ angiogenesis, GO:0048514 ~ blood vessel morphogenesis.

For 9527 treatment, 11 terms are upregulated (Table 13). The prevailing terms are related to ribosome biogenesis, *e.g.*, GO:0042254 ~ ribosome biogenesis, GO:0022613 ~ ribonucleoprotein complex biogenesis and GO:0006364 ~ rRNA processing.

Table 3
Response genes in 9500 + oil treatment.

Ensembl ID	HGNC symbol	Raw p value	BH-adjusted p	log2 Fold Change
ENSG00000123689	G0S2	5.41E-07	0.004481	0.796118
ENSG00000144810	*COL8A1*	3.89E-06	0.021487	−0.60543
ENSG00000151892	GFRA1	1.91E-05	0.079212	−0.62845
ENSG00000203727	SAMD5	2.97E-05	0.098496	−0.73684

Note: COL8A1 is the response gene also for 9500 and 9527 + oil treatments.

Table 4
Response genes in 9527 + oil treatment vs. control.

Ensembl ID	HGNC symbol	Raw p value	BH-adjusted p	log2 fold change
ENSG00000144810	*COL8A1*	1.29E-12	1.72E-08	−0.66
ENSG00000128965	CHAC1	5.03E-11	3.35E-07	−0.74
ENSG00000169174	*PCSK9*	7.71E-11	3.42E-07	−0.71
ENSG00000104419	NDRG1	7.04E-09	2.34E-05	0.62
ENSG00000154678	PDE1C	1.80E-08	4.79E-05	−0.59
ENSG00000183691	NOG	1.56E-07	3.45E-04	−0.61
ENSG00000128342	LIF	2.53E-07	4.81E-04	−0.60
ENSG00000132003	*ZSWIM4*	5.44E-07	7.93E-04	−0.49
ENSG00000106366	SERPINE1	5.51E-07	7.93E-04	−0.56
ENSG00000142627	*EPHA2*	5.96E-07	7.93E-04	−0.42
ENSG00000149090	*PAMR1*	1.12E-06	1.36E-03	−0.48
ENSG00000137285	*TUBB2B*	1.65E-06	1.80E-03	−0.37
ENSG00000138764	CCNG2	1.76E-06	1.80E-03	0.46
ENSG00000138166	DUSP5	4.17E-06	3.70E-03	−0.54
ENSG00000149571	*KIRREL3*	5.40E-06	4.49E-03	−0.50
ENSG00000148677	ANKRD1	6.12E-06	4.79E-03	−0.50
ENSG00000181649	PHLDA2	1.10E-05	7.70E-03	−0.42
ENSG00000139178	C1RL	1.25E-05	8.32E-03	0.39
ENSG00000123405	NFE2	1.94E-05	1.23E-02	0.49
ENSG00000149591	*TAGLN*	2.34E-05	1.41E-02	−0.39
ENSG00000224389	C4B	2.52E-05	1.41E-02	0.35
ENSG00000159403	*C1R*	2.54E-05	1.41E-02	0.35
ENSG00000155324	GRAMD3	2.90E-05	1.54E-02	−0.46
ENSG00000112658	SRF	3.43E-05	1.75E-02	−0.35
ENSG00000169242	EFNA1	3.97E-05	1.96E-02	0.42
ENSG00000125726	CD70	4.30E-05	2.04E-02	−0.45
ENSG00000113070	HBEGF	5.82E-05	2.67E-02	−0.47
ENSG00000107159	CA9	6.24E-05	2.77E-02	0.45
ENSG00000167470	MIDN	9.37E-05	3.89E-02	−0.35
ENSG00000106772	PRUNE2	1.11E-04	4.49E-02	−0.45
ENSG00000160932	*LY6E*	1.39E-04	5.43E-02	0.31
ENSG00000198910	L1CAM	1.61E-04	6.13E-02	−0.43
ENSG00000223749	MIR503HG	1.76E-04	6.52E-02	−0.41
ENSG00000149451	ADAM33	2.00E-04	7.19E-02	−0.36
ENSG00000150782	IL18	2.06E-04	7.21E-02	−0.35
ENSG00000205403	CFI	2.22E-04	7.30E-02	0.42
ENSG00000120885	CLU	2.24E-04	7.30E-02	−0.30
ENSG00000225383	SFTA1P	2.25E-04	7.30E-02	−0.37
ENSG00000176171	BNIP3	2.40E-04	7.59E-02	0.31
ENSG00000113389	NPR3	2.92E-04	9.05E-02	−0.33
ENSG00000261801	LOXL1-AS1	3.07E-04	9.29E-02	−0.36
ENSG00000171617	ENC1	3.35E-04	9.68E-02	−0.36
ENSG00000148700	ADD3	3.41E-04	9.68E-02	0.34
ENSG00000070756	PABPC1	3.42E-04	9.68E-02	0.33
ENSG00000187678	SPRY4	3.61E-04	9.86E-02	−0.39
ENSG00000101443	*WFDC2*	3.74E-04	9.94E-02	0.41

Note: Genes with symbols italicized are those that also responded to other treatments. PCSK9, KIRREL3, C1R, TAGLN, LY6E and WFDC2 are the response genes also for 9500 treatment. ZSWIM4, HBEGF and EPHA2 are the response genes also for oil treatment. PAMR1 and TUBB2B are the response genes also for oil and 9500 treatments. COL8A1 is the response gene also for 9500 and 9500 + oil treatments.

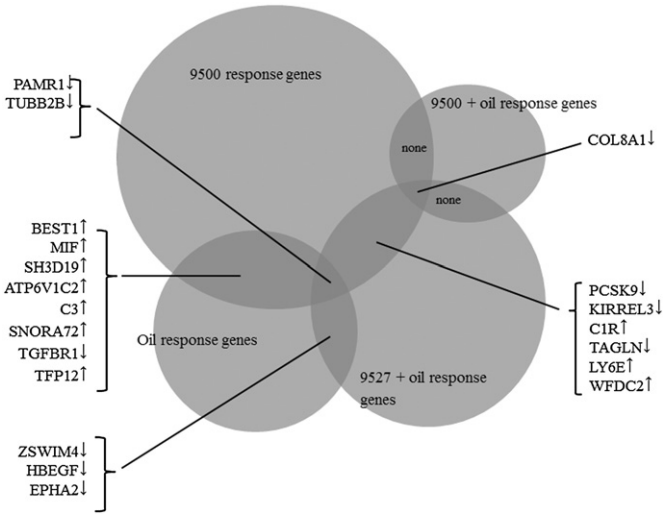

Fig. 3. Shared response genes among different treatments.

For 9527 + oil treatment, 12 terms are upregulated (Table 14). The prevailing terms are related to glycolysis and gluconeogenesis.

As examples, the genes that were counted into the four key functional terms, GO:0005912 ~ adherens junction, GO:0001568 ~ blood vessel development/GO:0001944 ~ vasculature development, and GO:0016126 ~ sterol biosynthetic process, are listed in Table 15.

3.2.3. GAGE analysis for gene sets related to immune and inflammatory response

We used another software package, GAGE (Luo et al., 2009), to perform gene-set-based differential expression analysis to identify pathways/gene sets up- or downregulated by the various treatments. Interestingly, those GO terms that are related to inflammatory response and immune response were also detected by GAGE as prevailing upregulated terms for 9500 treatment (Table 16). Shown in Table 16 are the top significant upregulated GO terms (with a BH-adjusted p value < 0.10) in the 9500 treatment. The majority of the terms are related to inflammatory response (*e.g.*, GO:0006954 inflammatory response, GO:0050727 regulation of inflammatory response, GO:0002526 acute inflammatory response, GO:0031347 regulation of defense response) and immune response (*e.g.*, GO:0045087 innate immune response, GO:0006958 complement activation, classical pathway, GO:0006956 complement activation, GO:0006959 humoral immune response, and GO:0002253 activation of immune response). For other treatments, such as oil treatment, 9527 + oil treatment, and 9500 + oil treatment, the similar terms were also among the top significant upregulated ones, although the p values were not as significant as for the 9500 treatment. Specifically, for the oil treatment, among the top 5 significant upregulated terms are GO:0050727 regulation of inflammatory response (p = 4.76E-3), GO:0006954 inflammatory response (p = 9.64E-3), GO:0002526 acute inflammatory response (p = 1.15E-2), and GO:0002673 regulation of acute inflammatory response (p = 1.21E-2). For the 9527 + oil treatment, the following terms achieved p values from 1.67E-3 to 3.80E-3, which are GO:0019724 B cell mediated immunity, GO:0030449 regulation of complement activation, GO:0045087 innate immune response, GO:0006956 complement activation, and GO:0006958 complement activation, classical pathway. For the 9500 + oil treatment, the term GO:0006954 inflammatory response is upregulated with a p value of 0.026. Overall, upregulated immune response and inflammatory response gene sets were detected as the key transcriptomic feature for various treatments, especially the 9500 treatment. This finding is consistent with that obtained through the DAVID analysis of the shared response genes for various treatments (Fig. 3 and Table 5).

4. Discussion

In the first study of RNA-seq analysis of human airway epithelial cells under the treatment of oil and/or dispersants, we identified some interesting findings on the cell behavior from the perspective of transcriptomics.

First, the effects of oil and dispersants 9500 and 9527 were different. At the individual gene level, 9500 alone appeared to have the largest effect, evidenced by 84 response genes as result of the treatment (Table 2). In contrast, 9527 alone appeared to have the weakest effect, evidenced by no response gene (no gene differentially expressed in treatment vs. control at the significance level of BH-adjusted p value of 0.10). Oil treatment had the medium-sized effect, with 26 response genes (Table 1).

Through analyzing 9500 + oil and 9527 + oil treatments, we identified interaction effects between the two dispersants and oil. Although 9527 alone had the weakest effect (no response gene detected for 9527 treatment alone), there were 46 response genes as a result of 9527 + oil treatment (Table 4). Although 9500 alone had the strongest effect (84 response genes for 9500 treatment), there were only 4 response genes as a result of 9500 + oil treatment (Table 3). Oil treatment alone resulted in 26 response genes (Table 1), which is also quite different from the 46 response genes for 9527 + oil treatment and the 4 response genes for 9500 + oil treatment. Such a difference in number of response genes (hence the size of treatment effects) between oil/dispersant treatment alone and "oil + dispersant" treatment suggested an interaction between oil and dispersants 9500 and 9527 in transcriptomic perturbation of human airway epithelial cells. As suggested in the above result, the effect of 9500 may be neutralized by oil when they are mixed together, while the effect of 9527 and oil may synergize with each other so as to produce an effect that was much stronger than when they were used alone.

Although in total there are 160 response genes as a result of oil/dispersant or "oil + dispersant" treatments (Tables 1-4), one eighth (20 genes, including 10 upregulated and 10 downregulated genes) of such genes overlap between different treatments (Fig. 3), suggesting existence of a shared, core set of genes/pathways, and the related common physiological processes in response to the stimulation of oil and dispersants. In particular, COL8A1 was downregulated in both 9500, 9500 + oil, and 9527 + oil treatments, and PAMR1 and TUBB2B were downregulated in both 9500, oil, and 9527 + oil treatments. Interestingly, the PAMR1 (peptidase domain containing associated with muscle regeneration 1) gene has been associated with bronchopulmonary dysplasia in a genome-wide association study (Wang et al., 2013), suggesting its important role in respiratory physiology and corroborating its identity as a core response gene in our study. Furthermore, recent

Table 5
DAVID functional annotation of the 10 upregulated response genes shared between different treatments.

Category	Term	Counted genes	%	Fold enrichment	Raw p value	BH-adjusted p value
SP_PIR_KEYWORDS	innate immunity	C3, C1R, MIF	33.33	92.48	3.36E-04	0.02
BIOCARTA	h_classicPathway: Classical Complement Pathway	C3, C1R	22.22	119.75	8.35E-03	0.04
SP_PIR_KEYWORDS	immune response	C3, C1R, MIF	33.33	32.20	2.73E-03	0.07

Note: The 10 shared upregulated response genes submitted to DAVID functional annotation analysis are BEST1, MIF, SH3D19, ATP6V1C2, C3, SNORA72, TFP12, C1R, LY6E, and WFDC2, as shown in Fig. 3.

Table 6
Significant GO or other functional terms down-regulated by oil treatment.

Category	Term	Count	%	Fold enrichment	Raw p value	Bonferroni corrected p value
GOTERM_CC_FAT	*GO:0005912 ~ adherens junction*	13	8.39	11.28	1.34E-09	2.61E-07
SP_PIR_KEYWORDS	phosphoprotein	91	58.71	1.64	3.86E-09	8.42E-07
GOTERM_CC_FAT	*GO:0070161 ~ anchoring junction*	13	8.39	10.17	4.40E-09	8.58E-07
GOTERM_CC_FAT	GO:0016323 ~ basolateral plasma membrane	12	7.74	7.95	2.70E-07	5.27E-05
UP_SEQ_FEATURE	compositionally biased region: Ser-rich	17	10.97	5.24	1.52E-07	8.12E-05
GOTERM_CC_FAT	*GO:0030055 ~ cell-substrate junction*	9	5.81	10.81	1.61E-06	3.14E-04
GOTERM_CC_FAT	GO:0005856 ~ cytoskeleton	27	17.42	2.63	4.41E-06	8.59E-04
GOTERM_CC_FAT	*GO:0030054 ~ cell junction*	16	10.32	4.16	5.16E-06	1.01E-03
GOTERM_CC_FAT	*GO:0005913 ~ cell-cell adherens junction*	6	3.87	23.07	5.27E-06	1.03E-03
SP_PIR_KEYWORDS	cytoskeleton	18	11.61	3.70	6.87E-06	1.50E-03
GOTERM_CC_FAT	*GO:0005925 ~ focal adhesion*	8	5.16	10.55	9.71E-06	1.89E-03
GOTERM_CC_FAT	*GO:0005924 ~ cell-substrate adherens junction*	8	5.16	10.15	1.25E-05	2.44E-03
GOTERM_CC_FAT	GO:0001725 ~ stress fiber	5	3.23	28.03	2.60E-05	5.06E-03
GOTERM_CC_FAT	GO:0032432 ~ actin filament bundle	5	3.23	25.87	3.62E-05	7.04E-03
GOTERM_CC_FAT	GO:0042641 ~ actomyosin	5	3.23	24.92	4.23E-05	8.21E-03
GOTERM_CC_FAT	GO:0031252 ~ cell leading edge	8	5.16	7.80	6.88E-05	1.33E-02
GOTERM_CC_FAT	GO:0001726 ~ ruffle	6	3.87	12.05	1.30E-04	2.51E-02
GOTERM_BP_FAT	GO:0007167 ~ enzyme linked receptor protein signaling pathway	13	8.39	4.51	2.81E-05	3.36E-02
SP_PIR_KEYWORDS	LIM domain	6	3.87	11.06	2.05E-04	4.37E-02

Note: Terms italicized are those that are shared between different treatments or mentioned in Result and Discussion.

Table 7
Significant GO or other functional terms downregulated by 9500 treatment.

Category	Term	Count	%	Fold Enrichment	Raw p value	Bonferroni corrected p value
SP_PIR_KEYWORDS	phosphoprotein	208	57.14	1.60	1.07E-17	3.75E-15
SP_PIR_KEYWORDS	actin-binding	23	6.32	5.19	7.04E-10	2.48E-07
GOTERM_BP_FAT	*GO:0016125 ~ sterol metabolic process*	17	4.67	8.19	2.08E-10	3.91E-07
SP_PIR_KEYWORDS	*Steroid biosynthesis*	11	3.02	15.33	1.55E-09	5.44E-07
SP_PIR_KEYWORDS	lipid synthesis	15	4.12	8.53	2.21E-09	7.79E-07
GOTERM_BP_FAT	GO:0008203 ~ cholesterol metabolic process	16	4.40	8.46	5.10E-10	9.58E-07
GOTERM_MF_FAT	GO:0003779 ~ actin binding	27	7.42	4.04	2.88E-09	1.58E-06
GOTERM_BP_FAT	*GO:0016126 ~ sterol biosynthetic process*	11	3.02	15.29	1.29E-09	2.42E-06
SP_PIR_KEYWORDS	*sterol biosynthesis*	9	2.47	20.07	8.01E-09	2.82E-06
SP_PIR_KEYWORDS	Cholesterol biosynthesis	8	2.20	23.48	2.31E-08	8.12E-06
GOTERM_CC_FAT	*GO:0005912 ~ adherens junction*	17	4.67	5.72	4.28E-08	1.34E-05
GOTERM_BP_FAT	GO:0007010 ~ cytoskeleton organization	30	8.24	3.35	2.32E-08	4.36E-05
GOTERM_CC_FAT	*GO:0070161 ~ anchoring junction*	17	4.67	5.16	1.84E-07	5.77E-05
GOTERM_CC_FAT	GO:0005856 ~ cytoskeleton	55	15.11	2.08	1.87E-07	5.88E-05
GOTERM_BP_FAT	GO:0006695 ~ cholesterol biosynthetic process	9	2.47	16.84	3.17E-08	5.96E-05
GOTERM_CC_FAT	GO:0015629 ~ actin cytoskeleton	21	5.77	4.07	2.19E-07	6.87E-05
GOTERM_MF_FAT	GO:0008092 ~ cytoskeletal protein binding	31	8.52	3.00	1.40E-07	7.63E-05
GOTERM_CC_FAT	GO:0042641 ~ actomyosin	8	2.20	15.46	5.43E-07	1.71E-04
GOTERM_BP_FAT	GO:0030029 ~ actin filament-based process	21	5.77	4.24	1.17E-07	2.20E-04
GOTERM_BP_FAT	*GO:0008202 ~ steroid metabolic process*	19	5.22	4.58	1.77E-07	3.32E-04
GOTERM_BP_FAT	GO:0030036 ~ actin cytoskeleton organization	20	5.49	4.31	2.00E-07	3.76E-04
GOTERM_BP_FAT	GO:0007167 ~ enzyme linked receptor protein signaling pathway	24	6.59	3.41	5.84E-07	1.10E-03
GOTERM_MF_FAT	GO:0016717 ~ oxidoreductase activity, acting on paired donors, with oxidation of a pair of donors resulting in the reduction of molecular oxygen to two molecules of water	5	1.37	40.67	2.46E-06	1.35E-03
KEGG_PATHWAY	hsa00900:Terpenoid backbone biosynthesis	6	1.65	17.53	1.36E-05	1.44E-03
GOTERM_CC_FAT	GO:0001725 ~ stress fiber	7	1.92	15.22	4.59E-06	1.44E-03
SP_PIR_KEYWORDS	cytoskeleton	30	8.24	2.63	4.23E-06	1.49E-03
SP_PIR_KEYWORDS	actin binding	8	2.20	11.15	6.18E-06	2.17E-03
GOTERM_CC_FAT	GO:0032432 ~ actin filament bundle	7	1.92	14.05	7.60E-06	2.39E-03
SP_PIR_KEYWORDS	cytoplasm	93	25.55	1.56	6.98E-06	2.45E-03
KEGG_PATHWAY	*hsa00100:Steroid biosynthesis*	6	1.65	15.47	2.70E-05	2.86E-03
GOTERM_CC_FAT	GO:0016323 ~ basolateral plasma membrane	15	4.12	3.86	3.50E-05	1.09E-02
SP_PIR_KEYWORDS	disease mutation	52	14.29	1.82	3.28E-05	1.15E-02
GOTERM_CC_FAT	*GO:0005913 ~ cell-cell adherens junction*	7	1.92	10.43	4.64E-05	1.45E-02
UP_SEQ_FEATURE	short sequence motif:Histidine box-2	5	1.37	30.87	1.20E-05	1.57E-02
UP_SEQ_FEATURE	short sequence motif:Histidine box-3	5	1.37	30.87	1.20E-05	1.57E-02
UP_SEQ_FEATURE	short sequence motif:Histidine box-1	5	1.37	30.87	1.20E-05	1.57E-02
GOTERM_BP_FAT	*GO:0006694 ~ steroid biosynthetic process*	11	3.02	6.30	8.91E-06	1.66E-02
GOTERM_CC_FAT	*GO:0030054 ~ cell junction*	25	6.87	2.52	5.48E-05	1.71E-02
GOTERM_CC_FAT	*GO:0030055 ~ cell-substrate junction*	11	3.02	5.12	5.50E-05	1.71E-02
SP_PIR_KEYWORDS	acetylation	74	20.33	1.57	7.54E-05	2.62E-02
KEGG_PATHWAY	*hsa04520:Adherens junction*	9	2.47	5.12	3.07E-04	3.21E-02
GOTERM_CC_FAT	*GO:0005925 ~ focal adhesion*	10	2.75	5.11	1.42E-04	4.36E-02

Note: Terms italicized are those that are shared between different treatments or mentioned in Result and Discussion.

Table 8
Significant GO or other functional terms down-regulated by 9527 + oil treatment.

Category	Term	Count	%	Fold enrichment	Raw p value	Bonferroni corrected p value
GOTERM_CC_FAT	GO:0044421 ~ extracellular region part	40	13.51	2.64	3.08E-08	8.69E-06
SP_PIR_KEYWORDS	cleavage on pair of basic residues	16	5.41	4.06	1.06E-05	3.58E-03
GOTERM_CC_FAT	GO:0005576 ~ extracellular region	56	18.92	1.76	1.59E-05	4.47E-03
SP_PIR_KEYWORDS	signal	76	25.68	1.61	1.64E-05	5.53E-03
GOTERM_BP_FAT	*GO:0051094 ~ positive regulation of developmental process*	18	6.08	3.89	3.82E-06	6.37E-03
GOTERM_BP_FAT	GO:0007167 ~ enzyme linked receptor protein signaling pathway	20	6.76	3.52	4.20E-06	6.99E-03
SP_PIR_KEYWORDS	phosphoprotein	140	47.30	1.32	2.39E-05	8.01E-03
GOTERM_CC_FAT	GO:0031012 ~ extracellular matrix	18	6.08	3.30	3.17E-05	8.90E-03
INTERPRO	IPR004827:Basic-leucine zipper (bZIP) transcription factor	8	2.70	9.71	1.65E-05	9.48E-03
GOTERM_BP_FAT	GO:0045597 ~ positive regulation of cell differentiation	16	5.41	4.20	6.31E-06	1.05E-02
SMART	SM00338:BRLZ	8	2.70	7.61	7.38E-05	1.07E-02
SP_PIR_KEYWORDS	cell adhesion	19	6.42	3.09	4.81E-05	1.61E-02
UP_SEQ_FEATURE	signal peptide	76	25.68	1.60	2.06E-05	2.00E-02
GOTERM_CC_FAT	GO:0005615 ~ extracellular space	26	8.78	2.40	7.35E-05	2.05E-02
UP_SEQ_FEATURE	domain:Fibronectin type-III 2	11	3.72	5.78	2.14E-05	2.08E-02
GOTERM_BP_FAT	GO:0030182 ~ neuron differentiation	22	7.43	3.02	1.26E-05	2.09E-02
UP_SEQ_FEATURE	domain:Fibronectin type-III 1	11	3.72	5.73	2.28E-05	2.22E-02
GOTERM_BP_FAT	*GO:0042127 ~ regulation of cell proliferation*	31	10.47	2.37	1.64E-05	2.71E-02
GOTERM_BP_FAT	*GO:0008284 ~ positive regulation of cell proliferation*	21	7.09	3.05	1.83E-05	3.01E-02
GOTERM_BP_FAT	GO:0043067 ~ regulation of programmed cell death	31	10.47	2.30	2.97E-05	4.84E-02

Note: Terms italicized are those that are shared between different treatments or mentioned in Results and Discussion.

data from breast carcinoma studies indicate that PAMR1 may have a role as tumor suppressor (Lo et al., 2015) and its downregulation as detected in our study may suggest contribution to tumorigenesis.

We submitted the 20 shared core genes (Fig. 3) to DAVID (Dennis et al., 2003) for functional annotation. Notably, for the 10 upregulated genes (BEST1, MIF, SH3D19, ATP6V1C2, C3, SNORA72, TFP12, C1R, LY6E, WFDC2), the top significant terms with BH-adjusted p value < 0.10 are innate immunity (C3, C1R, and MIF as counted genes), classical complement pathway (C3 and C1R as counted genes), and immune response (C3, C1R, and MIF as counted genes) (Table 5), suggesting an enhanced immune response and innate immunity as a core functional signature for the cells treated with oil and dispersants. This finding is supported by GAGE analysis (Luo et al., 2009), where a large number of gene sets related to immune response and inflammatory response were found upregulated in various treatment conditions, especially the 9500 treatment (Table 16).

To further annotate the response genes in different treatments at a more comprehensive scale, we submitted to DAVID (Dennis et al., 2003) those genes differentially expressed at the significance level of raw p value < 0.05. Here, downregulated genes were submitted separately from the upregulated ones so as to infer down- and upregulated terms/gene sets/pathways, respectively. The prevailing downregulated terms that were shared by different treatments (*i.e.*, oil and 9500 treatments) are cell junctions (including adherens junctions) (Tables 6–7), suggesting that the oil and 9500 treatments may weaken the cell junctions of airway epithelial cells. The prevailing upregulated terms shared in different treatments (i.e., 9500 and 9500 + oil treatments) (Tables 11–12) are related to vasculature development, suggesting that the treatments may promote angiogenesis in human airway epithelial cells. The findings here have major implications to the respiratory physiology. Cell junctions represent an essential part of the barrier to the outside world formed by airway epithelial cells, and disruption of these junctions or loss of junctional proteins has been found in asthma and cystic fibrosis patients (Georas and Rezaee, 2014; Heijink et al., 2014; Rezaee and Georas, 2014). As another key observation, enhanced airway angiogenesis has also been associated with asthma (Ribatti et al., 2009) and cystic fibrosis (Verhaeghe et al., 2007). Our findings of downregulated functional terms related to cell junctions (Tables 6-7) and upregulated functional terms related to angiogenesis (Tables 11–12) provided insights into the mechanistic basis for the observed respiratory symptoms(Zock et al., 2012) and airway oxidative stress (Rodriguez-Trigo et al., 2010) found in oil spill rescue workers. The enhanced terms of immune response and inflammatory response as detected by the DAVID analysis of the 10 upregulated genes shared in different treatments (Fig. 3 and Table 5) and GAGE analysis (Table 16) further consolidate this mechanistic basis since enhanced immune response is a well-known promoting factor for asthma (Holgate, 2012), chronic obstructive pulmonary disease (COPD) (Faner et al., 2013; Holtzman et al., 2014), and cystic fibrosis (Ratner and Mueller, 2012).

In addition, we observed several downregulated terms related to steroid biosynthesis in 9500 treatment (Table 7), suggesting attenuated steroid biosynthesis in human airway epithelial cells under

Table 9
Significant GO term down-regulated by 9527 treatment.

Category	Term	Count	%	Fold enrichment	Raw p value	Bonferroni-corrected p value
GOTERM_CC_FAT	GO:0044421 ~ extracellular region part	13	14.77	3.27	3.74E-04	4.24E-02

Table 10
Significant GO and other functional terms down-regulated by 9500 + oil treatment.

Category	Term	Count	%	Fold enrichment	Raw p value	Bonferroni corrected p value
SP_PIR_KEYWORDS	chondroitin sulfate proteoglycan	4	4.49	55.19	4.69E-05	7.89E-03
SP_PIR_KEYWORDS	signal	28	31.46	2.02	2.33E-04	3.86E-02
GOTERM_BP_FAT	GO:0008203 ~ cholesterol metabolic process	6	6.74	14.23	5.74E-05	3.89E-02

Table 11
Significant GO and other functional terms up-regulated by 9500 treatment.

Category	Term	Count	%	Fold enrichment	Raw p value	Bonferroni-corrected p value
GOTERM_CC_FAT	GO:0044421 ~ extracellular region part	36	12.63	2.37	2.26E-06	5.57E-04
GOTERM_CC_FAT	GO:0005576 ~ extracellular region	58	20.35	1.83	3.42E-06	8.44E-04
GOTERM_CC_FAT	GO:0005615 ~ extracellular space	28	9.82	2.59	9.43E-06	2.33E-03
GOTERM_BP_FAT	*GO:0001568 ~ blood vessel development*	17	5.96	4.27	2.38E-06	4.04E-03
GOTERM_BP_FAT	*GO:0001944 ~ vasculature development*	17	5.96	4.16	3.26E-06	5.53E-03
GOTERM_CC_FAT	GO:0022626 ~ cytosolic ribosome	9	3.16	7.03	3.92E-05	9.63E-03
SP_PIR_KEYWORDS	Secreted	45	15.79	1.91	3.47E-05	1.32E-02
SP_PIR_KEYWORDS	signal	72	25.26	1.59	3.99E-05	1.52E-02
SP_PIR_KEYWORDS	lysosome	11	3.86	5.30	4.51E-05	1.72E-02
KEGG_PATHWAY	hsa03010:Ribosome	9	3.16	5.54	1.78E-04	1.87E-02
SP_PIR_KEYWORDS	ribosome	8	2.81	7.87	6.85E-05	2.60E-02
SP_PIR_KEYWORDS	glycoprotein	88	30.88	1.46	8.21E-05	3.10E-02
UP_SEQ_FEATURE	signal peptide	72	25.26	1.58	4.92E-05	4.45E-02
GOTERM_CC_FAT	GO:0033279 ~ ribosomal subunit	10	3.51	4.94	1.87E-04	4.51E-02

Note: Terms italicized are those that are shared between different treatments or mentioned in Results and Discussion.

Table 12
Significant GO and other functional terms up-regulated by 9500 + oil treatment.

Category	Term	Count	%	Fold enrichment	Raw p value	Bonferroni-corrected p value
GOTERM_CC_FAT	GO:0044421 ~ extracellular region part	20	25.97	5.02	2.57E-09	3.37E-07
GOTERM_BP_FAT	*GO:0001568 ~ blood vessel development*	12	15.58	10.52	1.24E-08	1.01E-05
GOTERM_BP_FAT	*GO:0001944 ~ vasculature development*	12	15.58	10.27	1.59E-08	1.30E-05
GOTERM_CC_FAT	GO:0031012 ~ extracellular matrix	12	15.58	8.39	1.06E-07	1.39E-05
GOTERM_CC_FAT	GO:0005578 ~ proteinaceous extracellular matrix	11	14.29	8.29	5.23E-07	6.85E-05
SP_PIR_KEYWORDS	glycolysis	6	7.79	36.94	5.37E-07	9.77E-05
KEGG_PATHWAY	hsa00010:Glycolysis/Gluconeogenesis	6	7.79	19.56	8.56E-06	3.85E-04
GOTERM_CC_FAT	GO:0044420 ~ extracellular matrix part	7	9.09	14.43	7.47E-06	9.78E-04
GOTERM_CC_FAT	GO:0005581 ~ collagen	5	6.49	34.45	1.16E-05	1.52E-03
GOTERM_BP_FAT	GO:0006096 ~ glycolysis	6	7.79	27.41	2.27E-06	1.86E-03
GOTERM_CC_FAT	GO:0005576 ~ extracellular region	22	28.57	2.64	1.65E-05	2.16E-03
GOTERM_BP_FAT	*GO:0001525 ~ angiogenesis*	8	10.39	11.61	4.84E-06	3.95E-03
GOTERM_BP_FAT	*GO:0048514 ~ blood vessel morphogenesis*	9	11.69	9.16	5.03E-06	4.11E-03
GOTERM_BP_FAT	GO:0006007 ~ glucose catabolic process	6	7.79	22.21	6.52E-06	5.33E-03
GOTERM_BP_FAT	GO:0019320 ~ hexose catabolic process	6	7.79	18.67	1.54E-05	1.25E-02
GOTERM_BP_FAT	GO:0046365 ~ monosaccharide catabolic process	6	7.79	18.15	1.77E-05	1.44E-02
SP_PIR_KEYWORDS	Secreted	18	23.38	2.89	8.83E-05	1.59E-02
KEGG_PATHWAY	hsa00051:Fructose and mannose metabolism	4	5.19	23.01	5.68E-04	2.53E-02
GOTERM_BP_FAT	GO:0046164 ~ alcohol catabolic process	6	7.79	15.91	3.36E-05	2.72E-02
GOTERM_BP_FAT	GO:0044275 ~ cellular carbohydrate catabolic process	6	7.79	15.16	4.25E-05	3.42E-02
SP_PIR_KEYWORDS	extracellular matrix	7	9.09	7.87	2.44E-04	4.34E-02

Note: Terms italicized are those that are shared between different treatments or mentioned in Results and Discussion.

9500 stimulation. Steroid hormones are important for their potent anti-inflammatory and immunosuppressive effects. Local steroid hormone production was recently found in the mouse lung (Hostettler et al., 2012) and may represent a novel immunoregulatory mechanism to curb uncontrolled immune response in common lung diseases, such as asthma. Our findings here that suggested weakened steroid biosynthesis caused by 9500 treatment further revealed a functional insufficiency in 9500 treated airway epithelial cells that may place an exposed subject under a higher susceptibility to autoimmune-based lung diseases, such as asthma (Holgate, 2012) and COPD (Kheradmand et al., 2012).

Under each treatment, the cells were grown for 22 passages for ~3 months. This long-term exposure to treatment for ~3 months mimicked the length of time of the leakage of the sea floor oil gusher in the BP oil spill, which is also ~3 months, and hence the span of the period of "intense" exposure for those rescue workers when there was an "active"

Table 13
Significant GO and other functional terms up-regulated by 9527 treatment.

Category	Term	Count	%	Fold enrichment	Raw p value	Bonferroni-corrected p value
SP_PIR_KEYWORDS	rRNA processing	7	8.64	27.59	1.84E-07	3.30E-05
SP_PIR_KEYWORDS	acetylation	28	34.57	2.55	3.13E-06	5.63E-04
GOTERM_BP_FAT	GO:0042254 ~ ribosome biogenesis	8	9.88	15.04	8.38E-07	5.71E-04
GOTERM_BP_FAT	GO:0022613 ~ ribonucleoprotein complex biogenesis	9	11.11	11.46	9.14E-07	6.23E-04
GOTERM_CC_FAT	GO:0005730 ~ nucleolus	14	17.28	4.50	7.33E-06	9.52E-04
GOTERM_BP_FAT	GO:0006364 ~ rRNA processing	7	8.64	17.45	2.56E-06	1.74E-03
GOTERM_BP_FAT	GO:0016072 ~ rRNA metabolic process	7	8.64	16.72	3.28E-06	2.23E-03
GOTERM_BP_FAT	GO:0034660 ~ ncRNA metabolic process	9	11.11	8.97	5.70E-06	3.88E-03
SP_PIR_KEYWORDS	ribosome biogenesis	5	6.17	25.05	4.47E-05	8.01E-03
GOTERM_CC_FAT	GO:0030529 ~ ribonucleoprotein complex	11	13.58	4.79	6.92E-05	8.96E-03
SP_PIR_KEYWORDS	phosphoprotein	47	58.02	1.56	1.73E-04	3.07E-02

Table 14
Significant GO and other functional terms up-regulated by 9527 + oil treatment.

Category	Term	Count	%	Fold enrichment	Raw p value	Bonferroni-corrected p value
KEGG_PATHWAY	hsa00010:Glycolysis/Gluconeogenesis	9	4.00	11.92	5.43E-07	4.67E-05
GOTERM_BP_FAT	GO:0006096 ~ glycolysis	8	3.56	14.13	1.30E-06	1.57E-03
SP_PIR_KEYWORDS	glycolysis	7	3.11	14.10	9.25E-06	2.48E-03
GOTERM_CC_FAT	GO:0000796 ~ condensin complex	4	1.78	63.12	2.20E-05	4.59E-03
GOTERM_BP_FAT	GO:0006007 ~ glucose catabolic process	8	3.56	11.45	5.58E-06	6.70E-03
COG_ONTOLOGY	Chromatin structure and dynamics/Cell division and chromosome partitioning	3	1.33	60.94	7.27E-04	9.41E-03
SP_PIR_KEYWORDS	gluconeogenesis	5	2.22	23.33	5.25E-05	1.40E-02
INTERPRO	IPR015493:Protocadherin beta	5	2.22	25.65	3.47E-05	1.53E-02
KEGG_PATHWAY	hsa00030:Pentose phosphate pathway	5	2.22	15.89	2.23E-04	1.90E-02
GOTERM_BP_FAT	GO:0019320 ~ hexose catabolic process	8	3.56	9.62	1.79E-05	2.14E-02
GOTERM_BP_FAT	GO:0046365 ~ monosaccharide catabolic process	8	3.56	9.35	2.17E-05	2.58E-02
SMART	SM00244:PHB	4	1.78	25.87	4.18E-04	4.33E-02

Table 15
Component genes for some key response functional terms.

GO:0005912 ~ adherens junction	
ENSEMBL_GENE_ID	*Gene name*
ENSG00000072110	actinin, alpha 1
ENSG00000050405	LIM domain and actin binding 1
ENSG00000073712	fermitin family homolog 2 (Drosophila)
ENSG00000124145	syndecan 4
ENSG00000050820	similar to breast cancer anti-estrogen resistance 1; breast cancer anti-estrogen resistance 1
ENSG00000104067	tight junction protein 1 (zona occludens 1)
ENSG00000035403	vinculin
ENSG00000092295	transglutaminase 1 (K polypeptide epidermal type I, protein-glutamine-gamma-glutamyltransferase)
ENSG00000072163	LIM and senescent cell antigen-like domains 2
ENSG00000159840	zyxin
ENSG00000197694	spectrin, alpha, non-erythrocytic 1 (alpha-fodrin)
ENSG00000130202	poliovirus receptor-related 2 (herpesvirus entry mediator B)
ENSG00000164741	deleted in liver cancer 1
ENSG00000186575	neurofibromin 2 (merlin)
ENSG00000154380	enabled homolog (Drosophila)
ENSG00000057294	plakophilin 2
ENSG00000100345	myosin, heavy chain 9, non-muscle
GO:0001568 ~ blood vessel development/GO:0001944 ~ vasculature development	
ENSEMBL_GENE_ID	*Gene name*
ENSG00000105220	glucose phosphate isomerase
ENSG00000167772	angiopoietin-like 4
ENSG00000101384	jagged 1 (Alagille syndrome)
ENSG00000150630	vascular endothelial growth factor C
ENSG00000125538	interleukin 1, beta
ENSG00000135363	LIM domain only 2 (rhombotin-like 1)
ENSG00000112769	laminin, alpha 4
ENSG00000198959	transglutaminase 2 (C polypeptide, protein-glutamine-gamma-glutamyltransferase)
ENSG00000130203	hypothetical LOC100129500; apolipoprotein E
ENSG00000113083	lysyl oxidase
ENSG00000122861	plasminogen activator, urokinase
ENSG00000169855	roundabout, axon guidance receptor, homolog 1 (Drosophila); similar to roundabout 1 isoform b
ENSG00000171223	jun B proto-oncogene
ENSG00000142871	cysteine-rich, angiogenic inducer, 61
ENSG00000177606	jun oncogene
ENSG00000166825	alanyl (membrane) aminopeptidase
ENSG00000185650	zinc finger protein 36, C3H type-like 1
GO:0016126 ~ sterol biosynthetic process	
ENSEMBL_GENE_ID	*Name*
ENSG00000167508	mevalonate (diphospho) decarboxylase
ENSG00000147383	NAD(P) dependent steroid dehydrogenase-like
ENSG00000104549	squalene epoxidase
ENSG00000109929	sterol-C5-desaturase (ERG3 delta-5-desaturase homolog, S. cerevisiae)-like
ENSG00000067064	isopentenyl-diphosphate delta isomerase 1
ENSG00000160752	farnesyl diphosphate synthase (farnesyl pyrophosphate synthetase, dimethylallyltranstransferase, geranyltranstransferase)
ENSG00000112972	3-hydroxy-3-methylglutaryl-Coenzyme A synthase 1 (soluble)
ENSG00000116133	24-dehydrocholesterol reductase
ENSG00000172893	7-dehydrocholesterol reductase
ENSG00000113161	3-hydroxy-3-methylglutaryl-Coenzyme A reductase
ENSG00000160285	lanosterol synthase (2,3-oxidosqualene-lanosterol cyclase)

Note: The genes listed here are those that were differentially expressed with a significance level of $p < 0.05$ and counted into the GO term.

Table 16
Upregulated GO gene sets in 9500 treatment detected in GAGE analysis.

	Raw p value	BH-adjusted p value	Gene set size
GO:0006954 inflammatory response	2.60E-06	7.13E-03	434
GO:0045087 innate immune response	3.37E-06	7.13E-03	450
GO:0050727 regulation of inflammatory response	9.71E-06	1.37E-02	176
GO:0031347 regulation of defense response	2.00E-05	2.12E-02	387
GO:0019058 viral infectious cycle	3.63E-05	3.00E-02	191
GO:0006415 translational termination	5.08E-05	3.00E-02	67
GO:0002526 acute inflammatory response	5.66E-05	3.00E-02	99
GO:0006958 complement activation, classical pathway	5.67E-05	3.00E-02	25
GO:0006956 complement activation	7.65E-05	3.37E-02	38
GO:0045071 negative regulation of viral genome replication	8.77E-05	3.37E-02	29
GO:0048525 negative regulation of viral reproduction	8.77E-05	3.37E-02	29
GO:0070972 protein localization to endoplasmic reticulum	1.39E-04	4.90E-02	96
GO:0006614 SRP-dependent cotranslational protein targeting to membrane	1.55E-04	5.03E-02	81
GO:0045047 protein targeting to ER	1.81E-04	5.42E-02	82
GO:0072599 establishment of protein localization to endoplasmic reticulum	1.92E-04	5.42E-02	83
GO:0043901 negative regulation of multi-organism process	2.41E-04	6.37E-02	46
GO:0006613 cotranslational protein targeting to membrane	2.92E-04	7.26E-02	83
GO:0006959 humoral immune response	3.10E-04	7.27E-02	89
GO:0002253 activation of immune response	3.27E-04	7.27E-02	265
GO:0019724 B cell mediated immunity	3.99E-04	8.43E-02	84
GO:0050778 positive regulation of immune response	4.61E-04	9.29E-02	323
GO:0006414 translational elongation	5.12E-04	9.83E-02	80
GO:0002673 regulation of acute inflammatory response	5.38E-04	9.90E-02	51

oil spill. In the field of cell molecular analysis of the effects of exposure to oil spill, a design of chronic exposure (>6 days of exposure) was often used to mimic the accumulative effects of long-term exposure to spilled oil and oil-dispersant mixtures (Anderson et al., 2009; Brewton et al., 2013; Elarbaoui et al., 2015; Rowe et al., 2009), and to the best of our knowledge, our length of treatment time is among the longest in the field and hence may be advantageous in more accurately revealing the actual accumulative effects of oil spill.

We selected the BEAS-2B cells as our study model since these cells represent bronchial epithelial cells, which are the first line of airway cells interacting with inhaled agents. We chose this particular model system also because it has been previously shown that environmental exposures can induce cell transformation of these cells (Lu et al., 2015; Park et al., 2015; Son et al., 2012; Vales et al., 2015; Zhang et al., 2012). The BEAS-2B cells have been used for about 30 years in various biomedical research studies, including toxicological studies that tested chemicals, including organic, inorganic, and particular agents (Fuentes-Mattei et al., 2010; Garcia-Canton et al., 2013; Lansley, 2015; Rodrigues et al., 2009; Steerenberg et al., 1998; Sun et al., 1995; Verstraelen et al., 2014).

Furthermore, a study comparing expression profiles of 10 commonly used lung cells lines and four primary cultures of human bronchial epithelial cells found that the BEAS-2B cell lines exhibited the highest homology in gene expression pattern with primary cells and the lowest number of dysregulated genes compared with non-tumoral lung tissues (Courcot et al., 2012). Thus, the data support BEAS-2B cells as an ideal surrogate of primary airway epithelial cells for toxicological and pharmacological studies (Courcot et al., 2012).

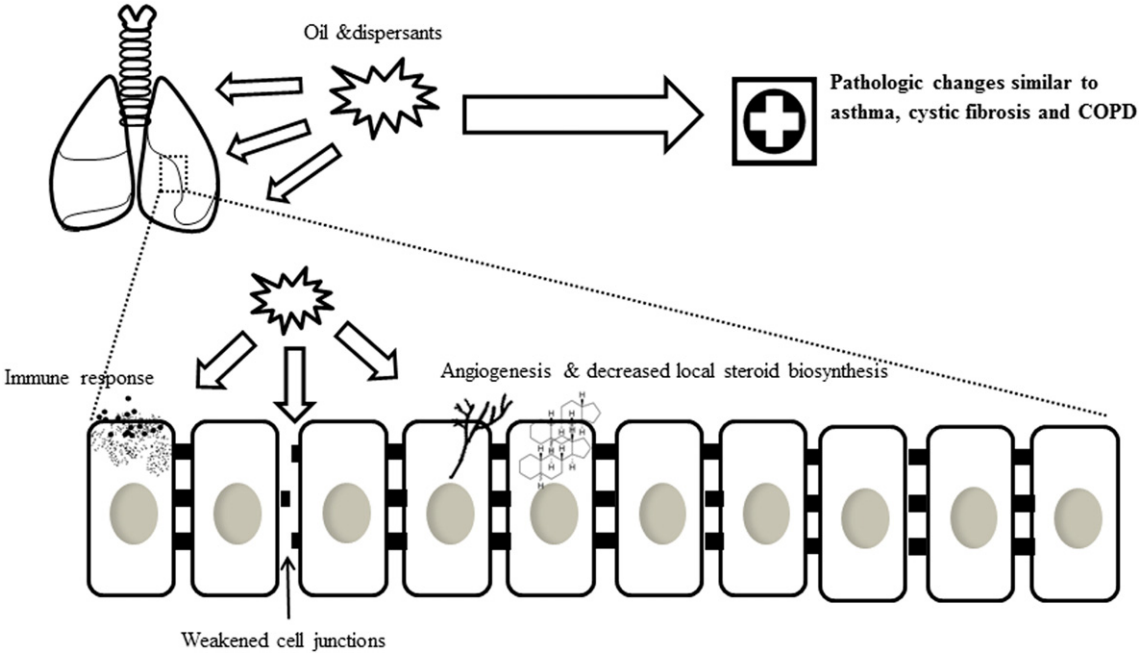

Fig. 4. Potential impacts of oil spill to lung health.

In addition, due to the high amount of available data using the BEAS-2B cell model, performing our experiments using this model would allow convenient comparison of our results with the existing data.

With regard to the submerged culture method, the method has been adopted by a large number of studies to analyze airway epithelial cells (Chu et al., 2015; Herzog et al., 2014; Kastner et al., 2013; Raemy et al., 2012). Importantly, compared with the air-liquid interface cell exposure (ALICE) system, submerged culture system is more suitable for modeling chronic exposure (Herzog et al., 2014), as the oil pollutants exposure scenario in our study. We did not use KGM but used DMEM as the culture medium because we carefully followed the culture medium condition (DMEM) that was previously reported for studying exposure-induced malignant transformation of the BEAS-2B cells (Huang et al., 2015; Kim et al., 2015; Liu et al., 2014; Park et al., 2015; Son et al., 2012; Stueckle et al., 2012). In addition, numerous studies (e.g., (Dieudonne et al., 2012; Jahn et al., 2000; Kaur et al., 2008; Skuland et al., 2014)) have used BEAS-2B cells cultured in DMEM as a model for airway epithelium. Therefore, our usage of DMEM as the culture medium for the BEAS-2B cells is consistent with the main purpose of our study and again, important for comparing our results with the published data.

Our findings, although functionally relevant and interesting, may need further replication using another independent biological sample set, ideally with a new run of RNA-seq experiments. The major aim of this study is not to evaluate molecular mechanisms but to identify the mode of action for airway epithelial cells to respond to oil-spill-related chemicals. The effects of the chemicals on gene expression in BEAS-2B cells identified in this study will provide evidence/basis for further validation using rigorous design and molecular techniques. Therefore, the mode of actions/mechanisms proposed in the study (Fig. 4) is expected to be verified by additional molecular biology and gene functional evidence.

5. Conclusion

In summary, we have performed the first RNA-seq-based transcriptome profiling study of human airway epithelial cells under treatments of crude oil and dispersants Corexit 9500 and Corexit 9527. Through differential expression analysis in treated cells vs. controls, we identified differentially expressed genes (response genes) in response to different treatments. Based on the number of differentially expressed genes at the significance level of BH-adjusted $p < 0.10$, 9500 has the strongest effect on transcriptomics perturbation while 9527 has the weakest effect. However, when mixed with oil, 9527 has a much stronger effect than 9527 alone, and 9500 has a much weaker effect than 9500 alone, suggesting interaction (synergizing or neutralizing) effects between oil and the two dispersants. More importantly, based on the annotation of the response genes, the response pathways/functional terms are characterized by enhanced angiogenesis and immune response and weakened cell junctions and steroid synthesis, and these signature pathways/gene sets correspond to some of the key pathological features for asthma, cystic fibrosis, or COPD. Based on these findings, we propose a working model for the effect of oil and dispersants to lung physiology at the airway epithelial cell level (Fig. 4). Our findings provide mechanistic insights into the pathophysiology of the lung diseases previously found in the oil spill rescue workers (Rodriguez-Trigo et al., 2010; Zock et al., 2012) and are valuable for assessing and modeling the potential health impact to those workers recently involved in the cleaning operation for the BP oil spill.

Acknowledgements

This study was supported by NIOSH (National Institute for Occupational Safety and Health) Pilot Projects Research Training Program of Southwest Center for Occupational and Environmental Health. AMR-E is also supported by the by National Institutes of Health (NIH) P20GM103518/ P20RR020152. Its contents are solely the responsibility of the authors and do not necessarily represent the official views of NIH.

References

Anderson, B.S., Arenella-Parkerson, D., Phillips, B.M., Tjeerdema, R.S., Crane, D., 2009. Preliminary investigation of the effects of dispersed Prudhoe ray crude oil on developing topsmelt embryos, *Atherinops affinis*. Environ. Pollut. 157 (3), 1058–1061.

Barron, M.G., Carls, M.G., Short, J.W., Rice, S.D., 2003. Photoenhanced toxicity of aqueous phase and chemically dispersed weathered Alaska North Slope crude oil to Pacific herring eggs and larvae. Environ. Toxicol. Chem. 22 (3), 650–660.

Benjamini, Y., Hochberg, Y., 1995. Controlling the false discovery rate: a practical and powerful approach to multiple testing. J. R. Stat. Soc. Ser. B 57, 289–300.

Brewton, R.A., Fulford, R., Griffitt, R.J., 2013. Gene expression and growth as indicators of effects of the BP deepwater horizon oil spill on spotted seatrout (*Cynoscion nebulosus*). J. Toxic. Environ. Health A 76 (21), 1198–1209.

Chu, H.W., Rios, C., Huang, C., Wesolowska-Andersen, A., Burchard, E.G., O'Connor, B.P., Fingerlin, T.E., Nichols, D., Reynolds, S.D., Seibold, M.A., 2015. CRISPR-Cas9-mediated gene knockout in primary human airway epithelial cells reveals a proinflammatory role for MUC18. Gene Ther.

Courcot, E., Leclerc, J., Lafitte, J.J., Mensier, E., Jaillard, S., Gosset, P., Shirali, P., Pottier, N., Broly, F., Lo-Guidice, J.M., 2012. Xenobiotic metabolism and disposition in human lung cell models: comparison with in vivo expression profiles. Drug Metab. Dispos. 40 (10), 1953–1965.

Dennis Jr., G., Sherman, B.T., Hosack, D.A., Yang, J., Gao, W., Lane, H.C., Lempicki, R.A., 2003. DAVID: Database for Annotation, Visualization, and Integrated discovery. Genome Biol. 4 (5), 3.

Dieudonne, A., Torres, D., Blanchard, S., Taront, S., Jeannin, P., Delneste, Y., Pichavant, M., Trottein, F., Gosset, P., 2012. Scavenger receptors in human airway epithelial cells: role in response to double-stranded RNA. PLoS ONE 7 (8), e41952.

Duarte, R.M., Honda, R.T., Val, A.L., 2010. Acute effects of chemically dispersed crude oil on gill ion regulation, plasma ion levels and haematological parameters in tambaqui (*Colossoma macropomum*). Aquat. Toxicol. 97 (2), 134–141.

Dunn, O.J., 1961. Multiple comparisons among means. J. Am. Stat. Assoc. 50 (293), 52–64.

Elarbaoui, S., Richard, M., Boufahja, F., Mahmoudi, E., Thomas-Guyon, H., 2015. Effect of crude oil exposure and dispersant application on meiofauna: an intertidal mesocosm experiment. Environ. Sci.: Processes Impacts 17 (5), 997–1004.

Faner, R., Cruz, T., Agusti, A., 2013. Immune response in chronic obstructive pulmonary disease. Expert. Rev. Clin. Immunol. 9 (9), 821–833.

Fuentes-Mattei, E., Rivera, E., Gioda, A., Sanchez-Rivera, D., Roman-Velazquez, F.R., Jimenez-Velez, B.D., 2010. Use of human bronchial epithelial cells (BEAS-2B) to study immunological markers resulting from exposure to PM(2.5) organic extract from Puerto Rico. Toxicol. Appl. Pharmacol. **243** (3), 381–389.

Garcia-Canton, C., Minet, E., Anadon, A., Meredith, C., 2013. Metabolic characterization of cell systems used in in vitro toxicology testing: lung cell system BEAS-2B as a working example. Toxicol. in Vitro 27 (6), 1719–1727.

Georas, S.N., Rezaee, F., 2014. Epithelial barrier function: at the front line of asthma immunology and allergic airway inflammation. J. Allergy Clin. Immunol. 134 (3), 509–520.

Hayworth, J.S., Clement, T.P., 2012. Provenance of Corexit-related chemical constituents found in nearshore and inland Gulf Coast waters. Mar. Pollut. Bull. 64 (10), 2005–2014.

Heijink, I., van Oosterhout, A., Kliphuis, N., Jonker, M., Hoffmann, R., Telenga, E., Klooster, K., Slebos, D.J., ten Hacken, N., Postma, D., van den Berge, M., 2014. Oxidant-induced corticosteroid unresponsiveness in human bronchial epithelial cells. Thorax 69 (1), 5–13.

Hemmer, M.J., Barron, M.G., Greene, R.M., 2011. Comparative toxicity of eight oil dispersants, Louisiana sweet crude oil (LSC), and chemically dispersed LSC to two aquatic test species. Environ. Toxicol. Chem. 30 (10), 2244–2252.

Herzog, F., Loza, K., Balog, S., Clift, M.J., Epple, M., Gehr, P., Petri-Fink, A., Rothen-Rutishauser, B., 2014. Mimicking exposures to acute and lifetime concentrations of inhaled silver nanoparticles by two different in vitro approaches. Beilstein J. Nanotechnol. 5, 1357–1370.

Holgate, S.T., 2012. Innate and adaptive immune responses in asthma. Nat. Med. 18 (5), 673–683.

Holtzman, M.J., Byers, D.E., Alexander-Brett, J., Wang, X., 2014. The role of airway epithelial cells and innate immune cells in chronic respiratory disease. Nat. Rev. Immunol. 14 (10), 686–698.

Hostettler, N., Bianchi, P., Gennari-Moser, C., Kassahn, D., Schoonjans, K., Corazza, N., Brunner, T., 2012. Local glucocorticoid production in the mouse lung is induced by immune cell stimulation. Allergy 67 (2), 227–234.

Huang, H., Pan, X., Jin, H., Li, Y., Zhang, L., Yang, C., Liu, P., Liu, Y., Chen, L., Li, J., Zhu, J., Zeng, X., Fu, K., Chen, G., Gao, J., Huang, C., 2015. PHLPP2 downregulation contributes to lung carcinogenesis following B[a]P/B[a]PDE exposure. Clin. Cancer Res. 21 (16), 3783–3793.

Jahn, H.U., Krull, M., Wuppermann, F.N., Klucken, A.C., Rosseau, S., Seybold, J., Hegemann, J.H., Jantos, C.A., Suttorp, N., 2000. Infection and activation of airway epithelial cells by *Chlamydia pneumoniae*. J. Infect. Dis. 182 (6), 1678–1687.

Kastner, P.E., Le, C.S., Zheng, W., Casset, A., Pons, F., 2013. A dynamic system for single and repeated exposure of airway epithelial cells to gaseous pollutants. Toxicol. in Vitro 27 (2), 632–640.

Kaur, M., Chivers, J.E., Giembycz, M.A., Newton, R., 2008. Long-acting beta2-adrenoceptor agonists synergistically enhance glucocorticoid-dependent

transcription in human airway epithelial and smooth muscle cells. Mol. Pharmacol. 73 (1), 203–214.
Kheradmand, F., Shan, M., Xu, C., Corry, D.B., 2012. Autoimmunity in chronic obstructive pulmonary disease: clinical and experimental evidence. Expert. Rev. Clin. Immunol. 8 (3), 285–292.
Kim, D., Dai, J., Fai, L.Y., Yao, H., Son, Y.O., Wang, L., Pratheeshkumar, P., Kondo, K., Shi, X., Zhang, Z., 2015. Constitutive activation of epidermal growth factor receptor promotes tumorigenesis of Cr(VI)-transformed cells through decreased reactive oxygen species and apoptosis resistance development. J. Biol. Chem. 290 (4), 2213–2224.
Kujawinski, E.B., Kido Soule, M.C., Valentine, D.L., Boysen, A.K., Longnecker, K., Redmond, M.C., 2011. Fate of dispersants associated with the deepwater horizon oil spill. Environ. Sci. Technol. 45 (4), 1298–1306.
Laffon, B., Fraga-Iriso, R., Perez-Cadahia, B., Mendez, J., 2006. Genotoxicity associated to exposure to Prestige oil during autopsies and cleaning of oil-contaminated birds. Food Chem. Toxicol. 44 (10), 1714–1723.
Lansley, A.B., 2015. Development of an absorption model using a human airway epithelial cell line. Eur. Respir. J. 6, 409S.
Lawrence, M., Huber, W., Pages, H., Aboyoun, P., Carlson, M., Gentleman, R., Morgan, M.T., Carey, V.J., 2013. Software for computing and annotating genomic ranges. PLoS Comput. Biol. 9 (8), e1003118.
Liu, W., Xiao, L., Dong, C., He, M., Pan, Y., Xie, Y., Tu, W., Fu, J., Shao, C., 2014. Long-term low-dose alpha-particle enhanced the potential of malignant transformation in human bronchial epithelial cells through MAPK/Akt pathway. Biochem. Biophys. Res. Commun. 447 (3), 388–393.
Lo, P.H., Tanikawa, C., Katagiri, T., Nakamura, Y., Matsuda, K., 2015. Identification of novel epigenetically inactivated gene PAMR1 in breast carcinoma. Oncol. Rep. 33 (1), 267–273.
Love, M.I., Huber, W., Anders, S., 2014. Moderated estimation of fold change and dispersion for RNA-seq data with DESeq2. Genome Biol. 15 (12), 550.
Lu, J., Zhang, M., Huang, Z., Sun, S., Zhang, Y., Zhang, L., Peng, L., Ma, A., Ji, P., Dai, J., Cui, T., Liu, H., Gao, J., 2015. SIRT1 in B[a]P-induced lung tumorigenesis. Oncotarget.
Luo, W., Friedman, M.S., Shedden, K., Hankenson, K.D., Woolf, P.J., 2009. GAGE: generally applicable gene set enrichment for pathway analysis. BMC Bioinf. 10, 161.
Major, D., Zhang, Q., Wang, G., Wang, H., 2012. Oil-dispersant mixtures: understanding chemical composition and its relation to human toxicity. Toxicol. Environ. Chem. 94 (9), 1832–1845.
Morgan, M., Pages, H., Obenchain, V., Hayden, N., 2010. Rsamtools: Binary Alignment (BAM), FASTA, Variant Call (BCF), and Tabix File Import Ref Type: Computer Program.
Park, Y.H., Kim, D., Dai, J., Zhang, Z., 2015. Human bronchial epithelial BEAS-2B cells, an appropriate in vitro model to study heavy metals induced carcinogenesis. Toxicol. Appl. Pharmacol. 287 (3), 240–245.
Perez-Cadahia, B., Lafuente, A., Cabaleiro, T., Pasaro, E., Mendez, J., Laffon, B., 2007. Initial study on the effects of Prestige oil on human health. Environ. Int. 33 (2), 176–185.
Perez-Cadahia, B., Laffon, B., Valdiglesias, V., Pasaro, E., Mendez, J., 2008a. Cytogenetic effects induced by Prestige oil on human populations: the role of polymorphisms in genes involved in metabolism and DNA repair. Mutat. Res. 653 (1–2), 117–123.
Perez-Cadahia, B., Mendez, J., Pasaro, E., Lafuente, A., Cabaleiro, T., Laffon, B., 2008b. Biomonitoring of human exposure to Prestige oil: effects on DNA and endocrine parameters. Environ. Health Insights. 2, 83–92.
Raemy, D.O., Grass, R.N., Stark, W.J., Schumacher, C.M., Clift, M.J., Gehr, P., Rothen-Rutishauser, B., 2012. Effects of flame made zinc oxide particles in human lung cells—a comparison of aerosol and suspension exposures. Part. Fibre Toxicol. 9, 33.
Ramachandran, S.D., Hodson, P.V., Khan, C.W., Lee, K., 2004. Oil dispersant increases PAH uptake by fish exposed to crude oil. Ecotoxicol. Environ. Saf. 59 (3), 300–308.
Ratner, D., Mueller, C., 2012. Immune responses in cystic fibrosis: are they intrinsically defective? Am. J. Respir. Cell Mol. Biol. 46 (6), 715–722.
Rezaee, F., Georas, S.N., 2014. Breaking barriers. New insights into airway epithelial barrier function in health and disease. Am. J. Respir. Cell Mol. Biol. **50** (5), 857–869.
Ribatti, D., Puxeddu, I., Crivellato, E., Nico, B., Vacca, A., Levi-Schaffer, F., 2009. Angiogenesis in asthma. Clin. Exp. Allergy 39 (12), 1815–1821.
Rodrigues, C.F., Urbano, A.M., Matoso, E., Carreira, I., Almeida, A., Santos, P., Botelho, F., Carvalho, L., Alves, M., Monteiro, C., Costa, A.N., Moreno, V., Alpoim, M.C., 2009. Human bronchial epithelial cells malignantly transformed by hexavalent chromium exhibit an aneuploid phenotype but no microsatellite instability. Mutat. Res. 670 (1–2), 42–52.
Rodrigues, R.V., Miranda-Filho, K.C., Gusmao, E.P., Moreira, C.B., Romano, L.A., Sampaio, L.A., 2010. Deleterious effects of water-soluble fraction of petroleum, diesel and gasoline on marine pejerrey *Odontesthes argentinensis* larvae. Sci. Total Environ. 408 (9), 2054–2059.
Rodriguez-Trigo, G., Zock, J.P., Pozo-Rodriguez, F., Gomez, F.P., Monyarch, G., Bouso, L., Coll, M.D., Verea, H., Anto, J.M., Fuster, C., Barbera, J.A., 2010. Health changes in fishermen 2 years after clean-up of the Prestige oil spill. Ann. Intern. Med. 153 (8), 489–498.
Rowe, C.L., Mitchelmore, C.L., Baker, J.E., 2009. Lack of biological effects of water accommodated fractions of chemically- and physically-dispersed oil on molecular, physiological, and behavioral traits of juvenile snapping turtles following embryonic exposure. Sci. Total Environ. 407 (20), 5344–5355.
Saeed, T., Al-Mutairi, M., 1999. Chemical composition of the water-soluble fraction of the leaded gasolines in seawater. Environ. Int. 25, 117–129.
Shi, Y., Roy-Engel, A.M., Wang, H., 2013. Effects of COREXIT dispersants on cytotoxicity parameters in a cultured human bronchial airway cells, BEAS-2B. J. Toxic. Environ. Health A 76 (13), 827–835.
Skuland, T., Ovrevik, J., Lag, M., Refsnes, M., 2014. Role of size and surface area for pro-inflammatory responses to silica nanoparticles in epithelial lung cells: importance of exposure conditions. Toxicol. in Vitro 28 (2), 146–155.
Son, Y.O., Wang, L., Poyil, P., Budhraja, A., Hitron, J.A., Zhang, Z., Lee, J.C., Shi, X., 2012. Cadmium induces carcinogenesis in BEAS-2B cells through ROS-dependent activation of PI3K/AKT/GSK-3beta/beta-catenin signaling. Toxicol. Appl. Pharmacol. 264 (2), 153–160.
Steerenberg, P.A., Zonnenberg, J.A., Dormans, J.A., Joon, P.N., Wouters, I.M., van Bree, L., Scheepers, P.T., Van Loveren, H., 1998. Diesel exhaust particles induced release of interleukin 6 and 8 by (primed) human bronchial epithelial cells (BEAS 2B) in vitro. Exp. Lung Res. 24 (1), 85–100.
Stueckle, T.A., Lu, Y., Davis, M.E., Wang, L., Jiang, B.H., Holaskova, I., Schafer, R., Barnett, J.B., Rojanasakul, Y., 2012. Chronic occupational exposure to arsenic induces carcinogenic gene signaling networks and neoplastic transformation in human lung epithelial cells. Toxicol. Appl. Pharmacol. 261 (2), 204–216.
Sun, W., Wu, R., Last, J.A., 1995. Effects of exposure to environmental tobacco smoke on a human tracheobronchial epithelial cell line. Toxicology 100 (1–3), 163–174.
Trapnell, C., Roberts, A., Goff, L., Pertea, G., Kim, D., Kelley, D.R., Pimentel, H., Salzberg, S.L., Rinn, J.L., Pachter, L., 2012. Differential gene and transcript expression analysis of RNA-seq experiments with TopHat and Cufflinks. Nat. Protoc. **7** (3), 562–578 PMCID: PMC3334321.
Vales, G., Rubio, L., Marcos, R., 2015. Long-term exposures to low doses of titanium dioxide nanoparticles induce cell transformation, but not genotoxic damage in BEAS-2B cells. Nanotoxicology 9, 568–578.
Verhaeghe, C., Tabruyn, S.P., Oury, C., Bours, V., Griffioen, A.W., 2007. Intrinsic pro-angiogenic status of cystic fibrosis airway epithelial cells. Biochem. Biophys. Res. Commun. 356 (3), 745–749.
Verstraelen, S., Remy, S., Casals, E., De, B.P., Witters, H., Gatti, A., Puntes, V., Nelissen, I., 2014. Gene expression profiles reveal distinct immunological responses of cobalt and cerium dioxide nanoparticles in two in vitro lung epithelial cell models. Toxicol. Lett. 228 (3), 157–169.
Wang, H., St Julien, K.R., Stevenson, D.K., Hoffmann, T.J., Witte, J.S., Lazzeroni, L.C., Krasnow, M.A., Quaintance, C.C., Oehlert, J.W., Jelliffe-Pawlowski, L.L., Gould, J.B., Shaw, G.M., O'Brodovich, H.M., 2013. A genome-wide association study (GWAS) for bronchopulmonary dysplasia. Pediatrics 132 (2), 290–297.
Zhang, T., Qi, Y., Liao, M., Xu, M., Bower, K.A., Frank, J.A., Shen, H.M., Luo, J., Shi, X., Chen, G., 2012. Autophagy is a cell self-protective mechanism against arsenic-induced cell transformation. Toxicol. Sci. 130 (2), 298–308.
Zock, J.P., Rodriguez-Trigo, G., Rodriguez-Rodriguez, E., Espinosa, A., Pozo-Rodriguez, F., Gomez, F., Fuster, C., Castano-Vinyals, G., Anto, J.M., Barbera, J.A., 2012. Persistent respiratory symptoms in clean-up workers 5 years after the Prestige oil spill. Occup. Environ. Med. 69 (7), 508–513.